



Palindrome-Mediated Translocations in Humans: A New Mechanistic Model for Gross Chromosomal Rearrangements

Hidehito Inagaki^{1,2}, Takema Kato¹, Makiko Tsutsumi¹, Yuya Ouchi², Tamae Ohye³ and Hiroki Kurahashi^{1,2*}

¹ Division of Molecular Genetics, Institute for Comprehensive Medical Science, Fujita Health University, Toyoake, Japan,

² Genome and Transcriptome Analysis Center, Fujita Health University, Toyoake, Japan, ³ Department of Molecular Laboratory Medicine, Faculty of Medical Technology, School of Health Science, Fujita Health University, Toyoake, Japan

OPEN ACCESS

Edited by:

Karen M. Vasquez,
The University of Texas at Austin, USA

Reviewed by:

Ruslan Sadreyev,
Howard Hughes Medical Institute,
USA
Albino Bacolla,
The University of Texas MD Anderson
Cancer Center, USA

*Correspondence:

Hiroki Kurahashi
kura@fujita-hu.ac.jp

Specialty section:

This article was submitted to
Bioinformatics and Computational
Biology,
a section of the journal
Frontiers in Genetics

Received: 06 May 2016

Accepted: 28 June 2016

Published: 12 July 2016

Citation:

Inagaki H, Kato T, Tsutsumi M,
Ouchi Y, Ohye T and Kurahashi H
(2016) Palindrome-Mediated
Translocations in Humans: A New
Mechanistic Model for Gross
Chromosomal Rearrangements.
Front. Genet. 7:125.
doi: 10.3389/fgene.2016.00125

Palindromic DNA sequences, which can form secondary structures, are widely distributed in the human genome. Although the nature of the secondary structure—single-stranded “hairpin” or double-stranded “cruciform”—has been extensively investigated *in vitro*, the existence of such unusual non-B DNA *in vivo* remains controversial. Here, we review palindrome-mediated gross chromosomal rearrangements possibly induced by non-B DNA in humans. Recent advances in next-generation sequencing have not yet overcome the difficulty of palindromic sequence analysis. However, a dozen palindromic AT-rich repeat (PATRR) sequences have been identified at the breakpoints of recurrent or non-recurrent chromosomal translocations in humans. The breakages always occur at the center of the palindrome. Analyses of polymorphisms within the palindromes indicate that the symmetry and length of the palindrome affect the frequency of the *de novo* occurrence of these palindrome-mediated translocations, suggesting the involvement of non-B DNA. Indeed, experiments using a plasmid-based model system showed that the formation of non-B DNA is likely the key to palindrome-mediated genomic rearrangements. Some evidence implies a new mechanism that cruciform DNAs may come close together first in nucleus and illegitimately joined. Analysis of PATRR-mediated translocations in humans will provide further understanding of gross chromosomal rearrangements in many organisms.

Keywords: palindrome, inverted repeat, cruciform, chromosomal translocation, gross chromosomal rearrangement

INTRODUCTION

DNA palindromes consist of two units of identical sequences connected in an inverted position with respect to each other. In palindromes, the sequences on the complementary strands read the same in either direction. In other words, the complementary sequence appears in the same strand in an inverted orientation. Palindromic DNA can consequently form specific tertiary structures,

Abbreviations: PATRR, palindromic AT-rich repeat.

namely, single-stranded “hairpin” or double-stranded “cruciform” DNA. Such unusual DNA tertiary structures are called non-B DNA structures (Sinden, 1994; Wang and Vasquez, 2014). These non-B DNA structures are presumed to be generated in a cell under specific situations, although their *in vivo* existence is still a controversial subject.

Hairpin structures can be formed when the double helix DNA is dissociated into single-stranded DNA molecules at the palindrome. Such single-stranded DNA might occur during DNA or RNA synthesis during replication or transcription. On the other hand, cruciform formation starts from unwinding of the center of the double-stranded palindromic DNA, followed by extrusion at the center of the palindrome to form an intra-strand base-pairing of each strand. As the DNA unwinds, the cruciform gets bigger. Cruciform formation requires an under-twisted state, that is, negative superhelicity, of the DNA. Such unusual DNA structure itself could have an impact on DNA replication, repair, transcription, or other important biological pathways (Inagaki and Kurahashi, 2013). The DNA regions that potentially form non-B DNA structures often manifest genomic instability that induces gross chromosomal rearrangements (Pearson et al., 2005; Tanaka et al., 2005; Maizels, 2006; Raghavan and Lieber, 2006; Mirkin, 2007; McMurray, 2010).

PALINDROME-MEDIATED CHROMOSOMAL TRANSLOCATIONS IN HUMAN SPERM

The best-studied palindromic sequences are the breakpoint sequences of the constitutional t(11;22)(q23;q11.2) translocation, a well-known recurrent non-Robertsonian translocation in humans. Balanced carriers are healthy but often have reproductive problems such as infertility, recurrent pregnancy loss, and offspring with Emanuel syndrome (Carter et al., 2009; Ohye et al., 2014; Emanuel et al., 2015). Breakpoint analysis of 11q23 and 22q11 revealed that these regions contain a large palindrome of hundreds of base pairs that is extremely AT-rich (Kurahashi et al., 2000a, 2007; Edlmann et al., 2001; Kurahashi and Emanuel, 2001a; Tapia-Páez et al., 2001). These so-called palindromic AT-rich repeats (PATRRs) have been identified at both breakpoints on chromosomes 11 and 22 and are named PATRR11 and PATRR22, respectively. These PATRRs have several features in common. Both are several hundred base pairs in length and have greater than 90% AT content. They manifest nearly perfect palindromes without spacer regions but share little homology between the two chromosomes.

The most prominent feature of the t(11;22) translocation is that *de novo* translocations frequently arise at a similar breakpoint location. Translocation-specific PCR with primers flanking the breakpoints on chromosomes 11 and 22 can detect all of the t(11;22) junction sequence in the translocation carriers (Kurahashi et al., 2000b). We performed PCR at the single-molecule detection level using sperm DNA from normal healthy men with the 46, XY karyotype as template. Some DNA aliquots tested positive for t(11;22)-specific PCR products

while others were negative, suggesting that the PCR detected *de novo* t(11;22) translocations (Kurahashi and Emanuel, 2001b). The frequency was about one in 10,000. However, when the DNA of blood cells or cheek swab cells from the same men was analyzed, no translocation could be found. Furthermore, all of the lymphoblastoid cell lines or cultured fibroblasts examined also tested negative in PCR analysis. These results imply that the t(11;22) translocation arises in a sperm-specific fashion. There is no evidence for the occurrence of the t(11;22) translocation during female gametogenesis because of the limited availability of human oocytes for testing. However, in *de novo* t(11;22) families, analysis of the parental origin of the translocation chromosomes using the polymorphic feature of PATRR11 and PATRR22 revealed that all of the *de novo* t(11;22) translocations were of paternal origin, supporting a hypothesized sperm-specific mechanism of t(11;22) translocation formation (Ohye et al., 2010).

DNA SECONDARY STRUCTURE IN THE PALINDROME: HAIRPIN OR CRUCIFORM

What is behind the sperm-specific occurrence of the PATRR-mediated translocation? It is not unreasonable to discuss the mechanism leading to the t(11;22) translocation in the context of DNA secondary structure. The DNA secondary structure at the PATRR is potentially evidenced by the fact that a polymorphism within the PATRR affects the *de novo* t(11;22) translocation frequency (Kato et al., 2006; Tong et al., 2010). PATRR11 and PATRR22 have size polymorphisms in the general population due to deletion within the palindromic region. Carriers with long symmetric alleles preferably produce *de novo* t(11;22) translocations more frequently than carriers with PATRR asymmetric arms. These data indirectly but strongly implicate the presence of DNA secondary structure during translocation formation.

One hypothesis to explain the sperm specificity of the t(11;22) translocation is that it develops during DNA replication. Sperm production involves many cell divisions, each requiring DNA replication. During DNA replication, single-stranded DNA is generated in the template DNA for the synthesis of not only the lagging strand DNA, but also the leading strand (Azeroglu et al., 2014). When the replication fork comes to the palindromic region, a long single-stranded DNA is formed, inducing the formation of a single-stranded hairpin structure. The stalling of the replication fork produces DNA breakage at the palindromic region that can potentially induce translocations.

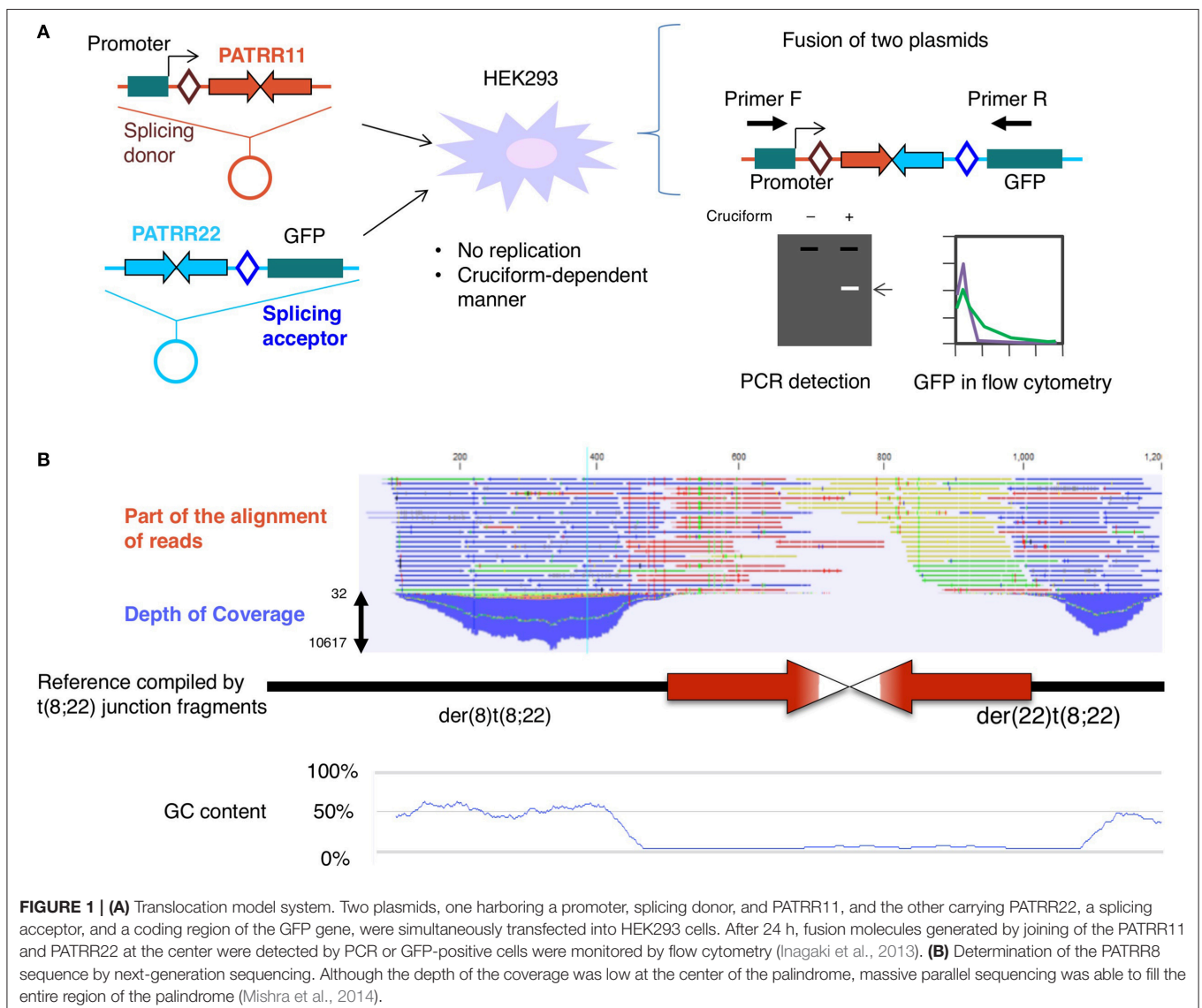
Because the germ stem cells in men replicate about 23 times per year, mature sperm from older men have undergone a greater number of replication cycles. The frequency of *de novo* point mutations in sperm cells increases according to the age of the sample donor (Crow, 2000; O’Roak et al., 2012). If the t(11;22) translocation is mediated by replication, the frequency of the *de novo* t(11;22) translocation should be higher in sperm from older men than in younger men for a similar reason. A previous analysis of the t(11;22) translocation

suggested, however, that there is no tendency for an increase in t(11;22) translocation frequency in the sperm of older men (Kato et al., 2007).

To determine the involvement of DNA replication in translocation formation, we established a model system for the t(11;22) translocation in cultured cells by using plasmids harboring PATRR11 or PATRR22 (Inagaki et al., 2009). Both plasmids were transfected into the HEK293 human cell line and we monitored the fusion of the different plasmids at each PATRR using GFP expression or translocation-specific PCR (Figure 1A). The results indicated that a translocation-like reaction took place. In this reaction, both PATRRs were cleaved at the center of the palindrome and joined via non-homologous end-joining in a similar manner to the human t(11;22) translocation. Crucially, the plasmids had no replication origin for human cells, which means that the translocation took place without DNA replication.

POST-MEIOSIS HYPOTHESIS FOR PATRR-MEDIATED TRANSLOCATIONS

On the other hand, it is possible that the translocation is mediated by another secondary structure, the DNA cruciform. In our model system, the plasmids were purified from *Escherichia coli* using a standard alkaline lysis method. Plasmid DNA isolated from *E. coli* has a strong negative superhelicity. If the plasmid has a palindromic region, the negative superhelicity facilitates cruciform extrusion (Kurahashi et al., 2004). Under an alkaline condition that induces denaturation of the plasmid DNA during purification, most of the PATRR-harboring plasmids extrude cruciform structures. Via the use of a non-denaturing condition and subsequent topoisomerase treatment, such superhelicity was relieved before cruciform extrusion. In this way, we can prepare different topoisomers of the same plasmid, both cruciform-extruded DNA and not extruded DNA. We tested the effect



of the cruciform on the translocation-like reaction in the cell using a mixture of cruciform and non-cruciform plasmids. The frequency of the translocation-like reaction was found to depend on the proportion of the cruciform-extruded plasmid DNA (Figure 1A; Inagaki et al., 2009). These results suggest that cruciform extrusion at the palindromic region induces PATRR-mediated translocation.

Notably however, in living cells the conversion of a DNA structure from that of standard B DNA to cruciform DNA is unlikely to occur under normal physiological conditions from a point of view of thermodynamics. Cruciform extrusion at the palindromic region occurs only when the DNA has strong free negative superhelicity. Theoretically, such superhelicity would potentially occur only at the post-meiosis stage in late spermatogenesis. At this developmental stage, histones are replaced by protamines to reduce the cell size (Gaucher et al., 2010). During histone removal, DNA has a transient excess of negative supercoiling, which might induce cruciform extrusion at the palindromic DNA that leads to translocation formation (Boissonneault, 2002). It is highly possible that PATRR-mediated translocations occur at this developmental stage of spermatogenesis (Kurahashi et al., 2010).

Although the post-meiosis hypothesis is captivating, there is some evidence contradicting this hypothesis. One example is the presence of somatic mosaicism of the t(11;22) translocation and normal cells in humans (Kurahashi et al., 2000b). This indicates that the t(11;22) translocation in this case was generated during the mitotic cell cycles after fertilization. Another example is the existence of *de novo* cases of Emanuel syndrome (Kurahashi et al., 2000b). Emanuel syndrome generally occurs via 3:1 segregation of the translocation chromosomes during meiosis I in a t(11;22) balanced carrier. However, a *de novo* Emanuel syndrome case would have arisen via 3:1 segregation of the t(11;22) chromosomes during the pre-meiotic somatic cell cycles of gametogenesis.

ANALYSIS OF THE PATRR BY NEXT-GENERATION SEQUENCING

In addition to PATRR11 and PATRR22, a dozen PATRRs have been found at other translocation breakpoints. A recurrent t(17;22)(q11.2;q11.2) translocation was found in neurofibromatosis type 1 patients (Kehrer-Sawatzki et al., 2002; Kurahashi et al., 2003). Identification of another recurrent translocation between 8q24.1 and 22q11.2 led to the definition of a new malformation syndrome (Sheridan et al., 2010). Other PATRRs at 4q35.1, 1p21.2, 3p14, and 9p21 were identified at the breakpoints of non-recurrent constitutional translocations (Nimmakayalu et al., 2003; Gotter et al., 2004; Tan et al., 2013; Kato et al., 2014). These PATRRs share little homology but have features of AT-richness and symmetric palindromic structure in common. Intriguingly, all of the palindrome-mediated translocations occur between one PATRR and another PATRR.

We attempted to perform genome-wide screening of *de novo* PATRR-mediated translocations to identify unknown PATRRs using next-generation sequencing. We used the PATRR22

sequence as bait for the detection of any unknown sequences next to the PATRR22 due to *de novo* translocation. However, several difficulties were encountered. We could not confirm the presence of the translocation because most of the PATRR-mediated non-recurrent translocations occurred at a frequency below the detection levels of PCR using sperm from normal healthy donors. Furthermore, we could not analyze the novel translocation junction because the partner sequence could not be mapped to the human reference sequence. None of the translocation-related PATRR sequences identified to date appear in the human genome assembly.

Although the genome projects for many organisms including humans determined their complete nucleotide sequences, difficult-to-sequence regions remain as “gaps.” Recent novel sequencing technologies have made it possible to access some of the gaps and provide more precise genomic data (Chaisson et al., 2015). The PATRR sequences do not appear even in such human reference databases. Palindrome sequences are one such type of a difficult-to-sequence region due to a “triple whammy” of factors affecting sequence analysis: the palindromic sequences are generally refractory to cloning to vectors, PCR amplification, and Sanger sequencing (Inagaki et al., 2005; Lewis et al., 2005). These features are due to the nature of the palindromic sequence itself. The longer the palindrome, the more difficult its analysis.

DEEP SEQUENCING OF THE PATRR REGION HAS GENERATED A NOVEL HYPOTHESIS

We applied next-generation sequencing technology to determine the complete sequence of the PATRR on 8q24, which was found at the breakpoint of t(8;22)(q24;q11) (Mishra et al., 2014). Sequencing of a random sheared library of PCR products and reconstruction of the original DNA via the computer-aided alignment of thousands of DNA molecules allowed us to successfully determine the entire PATRR8 (Figure 1B). The next-generation sequencing method does not require cloning and can directly analyze numerous DNA molecules at the same time. Although this strategy still requires PCR to amplify the single molecules and improve signal detection, the random digestion of the palindrome increases the chance of generating asymmetric cleavages of the palindromic center, which improves the PCR efficiency.

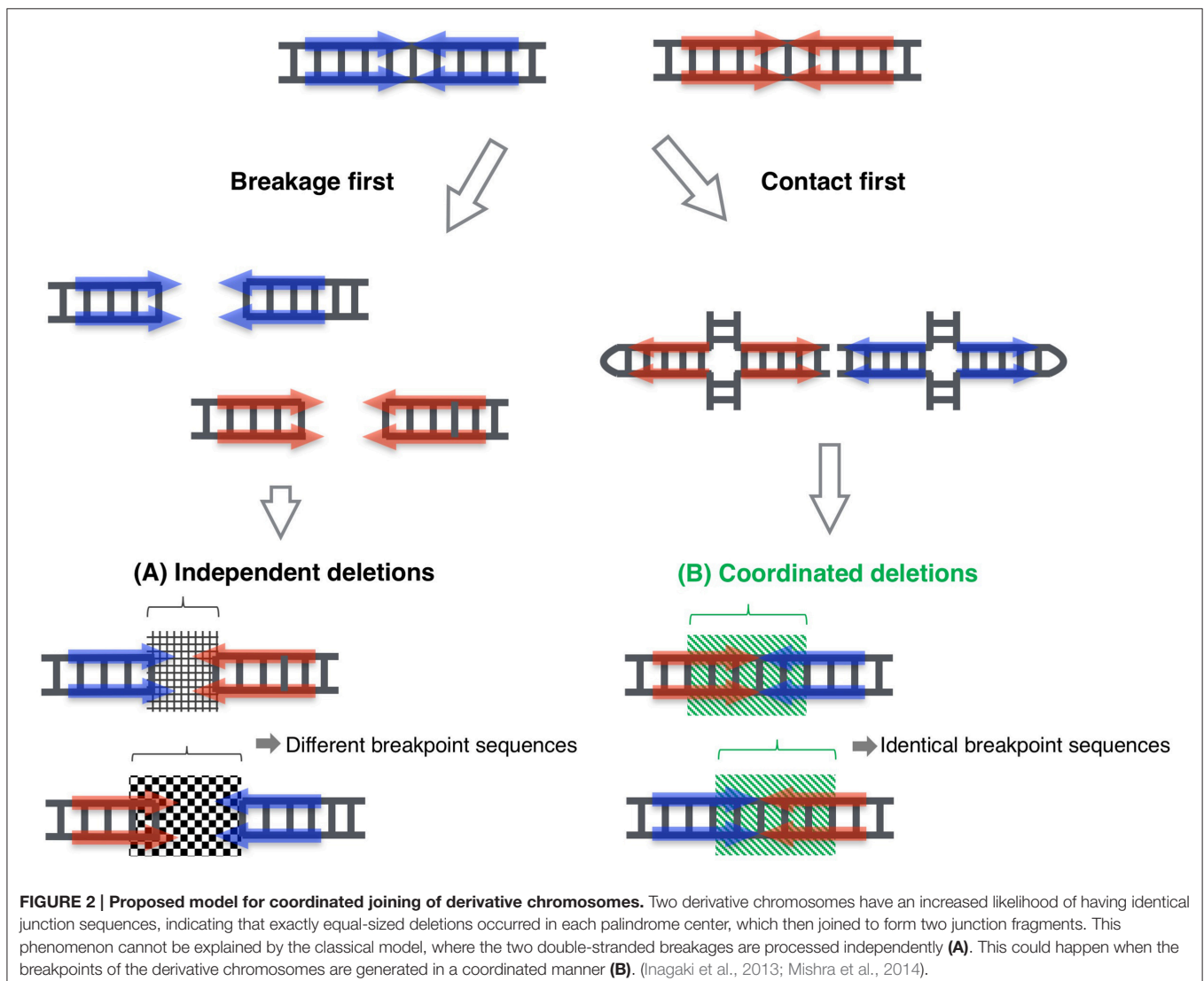
By means of this system, we determined the entire PATRR8 sequence, even at the center of the symmetry. This PATRR8 sequence allowed us to develop t(8;22)-specific PCR primers to analyze the junction fragments. The breakage always occurred at the center of the PATRR8 and PATRR22. The fusion was accompanied by the deletion of small nucleotides at the breakpoint regions. Interestingly, the nucleotide sequences around the junctions are identical between the der(8) and der(22) (Mishra et al., 2014). This cannot happen if the two breakages at the PATRR8 and PATRR22 occur independently and are followed by random nucleotide deletion at the breakage ends. This implies coordinated processing of PATRR8 and

PATRR22. Similar features of identical junctions in the two derivative chromosomes were also found in t(11;22) and t(17;22) (Kurahashi and Emanuel, 2001a; Kurahashi et al., 2003).

The standard models for gross chromosomal rearrangement include the breakage-first model and the contact-first model (Misteli and Soutoglou, 2009). In the breakage-first model, two DNA breaks located far from each other in the nucleus seek each other out to form a fusion chromosome. The artificial translocation model for the observation of the spatiotemporal chromosomal location in living cells revealed the dynamic movement of chromosomes after their breakage (Roukos et al., 2013). On the other hand, according to the contact-first model, translocation takes place between two closely located sites in the nucleus. Our previous data suggested that PATRR11 and PATRR22 are closer than other control chromosomal regions, indicating that this shorter distance might partly contribute to the recurrent nature of the t(11;22) translocation (Ashley et al., 2006). However, these

two models do not explain specific translocations between two PATRRs.

Again, the identical sequences of the two derivative chromosomes imply that the two DNA breakage sites are unlikely to have been processed independently. The two derivative chromosomes were likely to be generated in a coordinated manner. Taken together, in the case of a PATRR-mediated translocation, PATRR appears to extrude cruciform structures at some stage during spermatogenesis. The two cruciform DNA molecules seek each other out and finally join together (Figure 2). In our translocation model system in cultured cells described above, the data suggested that two cleavage processes—cleaved diagonal cleavage of the cruciform structure and cleavage of the tip of the hairpin structure—are involved in translocation development (Inagaki et al., 2013). Our data also suggest that the pathway involves the participation of Artemis and ligase IV, which are components of the V(D)J recombination system that act by bringing two chromosomal sites close together



and connecting them. In V(D)J recombination, RAG1 and RAG2 proteins bind the two cleavage sites to hold the resulting ends, both of which are specific for the V(D)J recombination machinery in lymphocytes. Similar mechanism is known in a DNA repair system of non-homologous end joining, in which Ku70/80 holds the two broken end until the subsequent repair machinery associate to process and join the ends (Deriano and Roth, 2013). Artemis and ligase IV as well as DNA-PK and other factors also participate in the joining reactions. It is possible that a part of such systems, or other novel factors might be involved in the contact between the two extruded cruciform structures and in keeping them in position during processing until the two derivative chromosomes are generated. We are now investigating how two cruciform DNA molecules come close together to elucidate the third mechanistic model that leads to recurrent chromosomal translocations in humans. Such investigation of dynamics of the cruciforms in nuclei will shed light on the role of non-B DNAs in gross chromosomal rearrangements in other eukaryotes.

REFERENCES

- Ashley, T., Gaeth, A. P., Inagaki, H., Seftel, A., Cohen, M. M., Anderson, L. K., et al. (2006). Meiotic recombination and spatial proximity in the etiology of the recurrent t(11;22). *Am. J. Hum. Genet.* 79, 524–538. doi: 10.1086/507652
- Azeroglu, B., Lincker, F., White, M. A., Jain, D., and Leach, D. R. (2014). A perfect palindrome in the *Escherichia coli* chromosome forms DNA hairpins on both leading- and lagging-strands. *Nucleic Acids Res.* 42, 13206–13213. doi: 10.1093/nar/gku1136
- Boissonneault, G. (2002). Chromatin remodeling during spermiogenesis: a possible role for the transition proteins in DNA strand break repair. *FEBS Lett.* 514, 111–114. doi: 10.1016/S0014-5793(02)02380-3
- Carter, M. T., St Pierre, S. A., Zackai, E. H., Emanuel, B. S., and Boycott, K. M. (2009). Phenotypic delineation of Emanuel syndrome (supernumerary derivative 22 syndrome): clinical features of 63 individuals. *Am. J. Med. Genet. A.* 149, 1712–1721. doi: 10.1002/ajmg.a.32957
- Chaisson, M. J., Huddleston, J., Dennis, M. Y., Sudmant, P. H., Malig, M., Hormozdiari, F., et al. (2015). Resolving the complexity of the human genome using single-molecule sequencing. *Nature* 517, 608–611. doi: 10.1038/nature13907
- Crow, J. F. (2000). The origins, patterns and implications of human spontaneous mutation. *Nat. Rev. Genet.* 1, 40–47. doi: 10.1038/35049558
- Deriano, L., and Roth, D. B. (2013). Modernizing the nonhomologous end-joining repertoire: alternative and classical NHEJ share the stage. *Annu. Rev. Genet.* 47, 433–455. doi: 10.1146/annurev-genet-110711-155540
- Edelmann, L., Spiteri, E., Koren, K., Pulijal, V., Bialer, M. G., Shanske, A., et al. (2001). AT-rich palindromes mediate the constitutional t(11;22) translocation. *Am. J. Hum. Genet.* 68, 1–13. doi: 10.1086/316952
- Emanuel, B. S., Zackai, E. H., and Medne, L. (2015). “Emanuel syndrome,” in *GeneReviews*, eds R. A. Pagon, M. P. Adam, H. H. Ardinger, S. E. Wallace, A. Amemiya, L. J. H. Bean, T. D. Bird, C. T. Fong, H. C. Mefford, R. J. H. Smith, and K. Stephens (Seattle, DC: University of Washington).
- Gaucher, J., Reynoird, N., Montellier, E., Bousouar, F., Rousseaux, S., and Khochbin, S. (2010). From meiosis to postmeiotic events: the secrets of histone disappearance. *FEBS J.* 277, 599–604. doi: 10.1111/j.1742-4658.2009.07504.x
- Gotter, A. L., Shaikh, T. H., Budarf, M. L., Rhodes, C. H., and Emanuel, B. S. (2004). A palindrome-mediated mechanism distinguishes translocations involving LCR-B of chromosome 22q11.2. *Hum. Mol. Genet.* 13, 103–115. doi: 10.1093/hmg/ddh004
- Inagaki, H., and Kurahashi, H. (2013). “Cruciform DNA,” in *Brenner’s Encyclopedia of Genetics, 2nd Edn.*, eds S. Maloy and K. Hughes (London, UK: Elsevier), 241–243.
- ## AUTHOR CONTRIBUTIONS
- HI and HK wrote the initial manuscript. All authors discussed the text and commented on the manuscript.
- ## FUNDING
- This study was supported by Grants-in-Aid for Scientific Research (HI, HK) and the MEXT-Supported Program for the Strategic Research Foundation at Private Universities (HK) from the Ministry of Education, Culture, Sports, Science, and Technology of Japan, and a Health and Labour Sciences Research Grant (HK) from the ministry of Health, Labour and Welfare of Japan.
- ## ACKNOWLEDGMENTS
- We thank Dr. Beverly S. Emanuel and the members of our laboratory for discussion and advice on this manuscript.
- Inagaki, H., Ohye, T., Kogo, H., Kato, T., Bolor, H., Taniguchi, M., et al. (2009). Chromosomal instability mediated by non-B DNA: cruciform conformation and not DNA sequence is responsible for recurrent translocation in humans. *Genome Res.* 19, 191–198. doi: 10.1101/gr.079244.108
- Inagaki, H., Ohye, T., Kogo, H., Tsutsumi, M., Kato, T., Tong, M., et al. (2013). Two sequential cleavage reactions on cruciform DNA structures cause palindrome-mediated chromosomal translocations. *Nat. Commun.* 4:1592. doi: 10.1038/ncomms2595
- Inagaki, H., Ohye, T., Kogo, H., Yamada, K., Kowa, H., Shaikh, T. H., et al. (2005). Palindromic AT-rich repeat in the NF1 gene is hypervariable in humans and evolutionarily conserved in primates. *Hum. Mutat.* 26, 332–342. doi: 10.1002/humu.20228
- Kato, T., Franconi, C. P., Sheridan, M. B., Hacker, A. M., Inagaki, H., Glover, T. W., et al. (2014). Analysis of the t(3;8) of hereditary renal cell carcinoma: a palindrome-mediated translocation. *Cancer Genet.* 207, 133–140. doi: 10.1016/j.cancergen.2014.03.004
- Kato, T., Inagaki, H., Yamada, K., Kogo, H., Ohye, T., Kowa, H., et al. (2006). Genetic variation affects *de novo* translocation frequency. *Science* 311, 971. doi: 10.1126/science.1121452
- Kato, T., Yamada, K., Inagaki, H., Kogo, H., Ohye, T., Emanuel, B. S., et al. (2007). Age has no effect on *de novo* constitutional t(11;22) translocation frequency in sperm. *Fertil. Steril.* 88, 1446–1448. doi: 10.1016/j.fertnstert.2007.01.019
- Kehrre-Sawatzki, H., Assum, G., and Hameister, H. (2002). Molecular characterisation of t(17;22)(q11.2;q11.2) is not consistent with NF1 gene duplication. *Hum. Genet.* 111, 465–467. doi: 10.1007/s00439-002-0794-3
- Kurahashi, H., and Emanuel, B. S. (2001a). Long AT-rich palindromes and the constitutional t(11;22) breakpoint. *Hum. Mol. Genet.* 10, 2605–2617. doi: 10.1093/hmg/10.23.2605
- Kurahashi, H., and Emanuel, B. S. (2001b). Unexpectedly high rate of *de novo* constitutional t(11;22) translocations in sperm from normal males. *Nat. Genet.* 29, 139–140. doi: 10.1038/ng1001-139
- Kurahashi, H., Inagaki, H., Hosoba, E., Kato, T., Ohye, T., Kogo, H., et al. (2007). Molecular cloning of a translocation breakpoint hotspot in 22q11. *Genome Res.* 17, 461–469. doi: 10.1101/gr.5769507
- Kurahashi, H., Inagaki, H., Ohye, T., Kogo, H., Tsutsumi, M., Kato, T., et al. (2010). The constitutional t(11;22): implications for a novel mechanism responsible for gross chromosomal rearrangements. *Clin. Genet.* 78, 299–309. doi: 10.1111/j.1399-0004.2010.01445.x
- Kurahashi, H., Inagaki, H., Yamada, K., Ohye, T., Taniguchi, M., Emanuel, B. S., et al. (2004). Cruciform DNA structure underlies the etiology for palindrome-mediated human chromosomal translocations. *J. Biol. Chem.* 279, 35377–35383. doi: 10.1074/jbc.M400354200

- Kurahashi, H., Shaikh, T. H., Hu, P., Roe, B. A., Emanuel, B. S., and Budarf, M. L. (2000a). Regions of genomic instability on 22q11 and 11q23 as the etiology for the recurrent constitutional t(11;22). *Hum. Mol. Genet.* 9, 1665–1670. doi: 10.1093/hmg/9.11.1665
- Kurahashi, H., Shaikh, T. H., Zackai, E. H., Celle, L., Driscoll, D. A., Budarf, M. L., et al. (2000b). Tightly clustered 11q23 and 22q11 breakpoints permit PCR-based detection of the recurrent constitutional t(11;22). *Am. J. Hum. Genet.* 67, 763–768. doi: 10.1086/303054
- Kurahashi, H., Shaikh, T., Takata, M., Toda, T., and Emanuel, B. S. (2003). The constitutional t(17;22): another translocation mediated by palindromic AT-rich repeats. *Am. J. Hum. Genet.* 72, 733–738. doi: 10.1086/368062
- Lewis, S. M., Chen, S., Strathern, J. N., and Rattray, A. J. (2005). New approaches to the analysis of palindromic sequences from the human genome: evolution and polymorphism of an intronic site at the NF1 locus. *Nucleic Acids Res.* 33, e186. doi: 10.1093/nar/gni189
- Maizels, N. (2006). Dynamic roles for G4 DNA in the biology of eukaryotic cells. *Nat. Struct. Mol. Biol.* 13, 1055–1059. doi: 10.1038/nsmb1171
- McMurray, C. T. (2010). Mechanisms of trinucleotide repeat instability during human development. *Nat. Rev. Genet.* 11, 786–799. doi: 10.1038/nrg2828
- Mirkin, S. M. (2007). Expandable DNA repeats and human disease. *Nature* 447, 932–940. doi: 10.1038/nature05977
- Mishra, D., Kato, T., Inagaki, H., Kosho, T., Wakui, K., Kido, Y., et al. (2014). Breakpoint analysis of the recurrent constitutional t(8;22)(q24.13;q11.21) translocation. *Mol. Cytogenet.* 7:55. doi: 10.1186/s13039-014-0055-x
- Misteli, T., and Soutoglou, E. (2009). The emerging role of nuclear architecture in DNA repair and genome maintenance. *Nat. Rev. Mol. Cell Biol.* 10, 243–254. doi: 10.1038/nrm2651
- Nimmakayalu, M. A., Gotter, A. L., Shaikh, T. H., and Emanuel, B. S. (2003). A novel sequence-based approach to localize translocation breakpoints identifies the molecular basis of a t(4;22). *Hum. Mol. Genet.* 12, 2817–2825. doi: 10.1093/hmg/ddg301
- Ohye, T., Inagaki, H., Kato, T., Tsutsumi, M., and Kurahashi, H. (2014). Prevalence of Emanuel syndrome: theoretical frequency and surveillance result. *Pediatr. Int.* 56, 462–466. doi: 10.1111/ped.12437
- Ohye, T., Inagaki, H., Kogo, H., Tsutsumi, M., Kato, T., Tong, M., et al. (2010). Paternal origin of the *de novo* constitutional t(11;22)(q23;q11). *Eur. J. Hum. Genet.* 18, 783–787. doi: 10.1038/ejhg.2010.20
- O’Roak, B. J., Vives, L., Girirajan, S., Karakoc, E., Krumm, N., Coe, B. P., et al. (2012). Sporadic autism exomes reveal a highly interconnected protein network of *de novo* mutations. *Nature* 485, 246–250. doi: 10.1038/nature10989
- Pearson, C. E., Edamura, K. N., and Cleary, J. D. (2005). Repeat instability: mechanisms of dynamic mutations. *Nat. Rev. Genet.* 6, 729–742. doi: 10.1038/nrg1689
- Raghavan, S. C., and Lieber, M. R. (2006). DNA structures at chromosomal translocation sites. *Bioessays* 28, 480–494. doi: 10.1002/bies.20353
- Roukos, V., Voss, T. C., Schmidt, C. K., Lee, S., Wangsa, D., and Misteli, T. (2013). Spatial dynamics of chromosome translocations in living cells. *Science* 341, 660–664. doi: 10.1126/science.1237150
- Sheridan, M. B., Kato, T., Haldeman-Englert, C., Jalali, G. R., Milunsky, J. M., Zou, Y., et al. (2010). A palindrome-mediated recurrent translocation with 3:1 meiotic nondisjunction: the t(8;22)(q24.13;q11.21). *Am. J. Hum. Genet.* 87, 209–218. doi: 10.1016/j.ajhg.2010.07.002
- Sinden, R. R. (1994). *DNA Structure and Function*. San Diego, CA: Academic Press.
- Tan, X., Anzick, S. L., Khan, S. G., Ueda, T., Stone, G., Digiovanna, J. J., et al. (2013). Chimeric negative regulation of p14ARF and TBX1 by a t(9;22) translocation associated with melanoma, deafness, and DNA repair deficiency. *Hum. Mutat.* 34, 1250–1259. doi: 10.1002/humu.22354
- Tanaka, H., Bergstrom, D. A., Yao, M. C., and Tapscott, S. J. (2005). Widespread and nonrandom distribution of DNA palindromes in cancer cells provides a structural platform for subsequent gene amplification. *Nat. Genet.* 37, 320–327. doi: 10.1038/ng1515
- Tapia-Páez, I., Kost-Alimova, M., Hu, P., Roe, B. A., Blennow, E., Fedorova, L., et al. (2001). The position of t(11;22)(q23;q11) constitutional translocation breakpoint is conserved among its carriers. *Hum. Genet.* 109, 167–177. doi: 10.1007/s004390100560
- Tong, M., Kato, T., Yamada, K., Inagaki, H., Kogo, H., Ohye, T., et al. (2010). Polymorphisms of the 22q11.2 breakpoint region influence the frequency of *de novo* constitutional t(11;22)s in sperm. *Hum. Mol. Genet.* 19, 2630–2637. doi: 10.1093/hmg/ddq150
- Wang, G., and Vasquez, K. M. (2014). Impact of alternative DNA structures on DNA damage, DNA repair, and genetic instability. *DNA Repair.* 19, 143–151. doi: 10.1016/j.dnarep.2014.03.017

Conflict of Interest Statement: The authors declare that the research was conducted in the absence of any commercial or financial relationships that could be construed as a potential conflict of interest.


Copyright © 2016 Inagaki, Kato, Tsutsumi, Ouchi, Ohye and Kurahashi. This is an open-access article distributed under the terms of the Creative Commons Attribution License (CC BY). The use, distribution or reproduction in other forums is permitted, provided the original author(s) or licensor are credited and that the original publication in this journal is cited, in accordance with accepted academic practice. No use, distribution or reproduction is permitted which does not comply with these terms.

CASE REPORT

Open Access



A case with concurrent duplication, triplication, and uniparental isodisomy at 1q42.12-qter supporting microhomology-mediated break-induced replication model for replicative rearrangements

Tomohiro Kohmoto^{1†}, Nana Okamoto^{2†}, Takuya Naruto¹, Chie Murata¹, Yuya Ouchi³, Naoko Fujita³, Hidehito Inagaki³, Shigeko Satomura⁴, Nobuhiko Okamoto⁵, Masako Saito¹, Kiyoshi Masuda¹, Hiroki Kurahashi³ and Issei Imoto^{1*} 

Abstract

Background: Complex genomic rearrangements (CGRs) consisting of interstitial triplications in conjunction with uniparental isodisomy (isoUPD) have rarely been reported in patients with multiple congenital anomalies (MCA)/intellectual disability (ID). One-ended DNA break repair coupled with microhomology-mediated break-induced replication (MMBIR) has been recently proposed as a possible mechanism giving rise to interstitial copy number gains and distal isoUPD, although only a few cases providing supportive evidence in human congenital diseases with MCA have been documented.

Case presentation: Here, we report on the chromosomal microarray (CMA)-based identification of the first known case with concurrent interstitial duplication at 1q42.12-q42.2 and triplication at 1q42.2-q43 followed by isoUPD for the remainder of chromosome 1q (at 1q43-qter). In distal 1q duplication/triplication overlapping with 1q42.12-q43, variable clinical features have been reported, and our 25-year-old patient with MCA/ID presented with some of these frequently described features. Further analyses including the precise mapping of breakpoint junctions within the CGR in a sequence level suggested that the CGR found in association with isoUPD in our case is a triplication with flanking duplications, characterized as a triplication with a particularly long duplication-inverted triplication-duplication (DUP-TRP/INV-DUP) structure. Because microhomology was observed in both junctions between the triplicated region and the flanking duplicated regions, our case provides supportive evidence for recently proposed replication-based mechanisms, such as MMBIR, underlying the formation of CGRs + isoUPD implicated in chromosomal disorders.

Conclusions: To the best of our knowledge, this is the first case of CGRs + isoUPD observed in 1q and having DUP-TRP/INV-DUP structure with a long proximal duplication, which supports MMBIR-based model for genomic rearrangements. Molecular cytogenetic analyses using CMA containing single-nucleotide polymorphism probes with further analyses of the breakpoint junctions are recommended in cases suspected of having complex chromosomal abnormalities based on discrepancies between clinical and conventional cytogenetic findings.

Keywords: 1q, Complex genomic rearrangement, Uniparental isodisomy, DUP-TRP/INV-DUP structure, Microhomology-mediated break-induced replication model, Template switching, Chromosomal microarray, Breakpoint junction sequence

* Correspondence: issehgen@tokushima-u.ac.jp

†Equal contributors

¹Department of Human Genetics, Graduate School of Biomedical Sciences, Tokushima University, 3-18-15 Kuramoto-cho, Tokushima 770-8503, Japan
Full list of author information is available at the end of the article

Background

Complex genomic rearrangements (CGRs) consisting of two or more breakpoint junctions have been frequently observed during the characterization of nonrecurrent microduplications associated with genomic disorders [1, 2]. The occurrence of CGRs, such as partial tetrasomy induced by an interstitial triplication, contiguous distally with an extended segment uniparental isodisomy (isoUPD), has recently been reported as a rare event [3–7]. The recent establishment of high-resolution chromosomal microarray (CMA) using probes designed to detect copy number variations (CNVs) and genotype single-nucleotide polymorphism (SNP) simultaneously in a genome-wide manner has accelerated the identification of cases with such CGRs + isoUPD observations [8]. Although the cause, mechanism, and phenotypic effect of such CGR + isoUPD remain unclear, Carvalho et al. [5] provided evidence that CGRs generated post-zygotically through microhomology-mediated break-induced replication (MMBIR) can lead to regional isoUPD. In this replication-based mechanism model, a triplicated segment inserted in an inverted orientation between two copies of the duplicated segments (duplication-inverted triplication-duplication, DUP-TRP/INV-DUP) followed by regional isoUPD is generated via template switches between homologs and sister chromatids using MMBIR [5].

Here, we report on a patient with the co-occurrence of interstitial trisomy at 1q42.12-q42.2 and tetrasomy at 1q42.2-q43, followed by a segmental isoUPD for 1q43-qter, as additional evidence for an MMBIR-based model generating DUP-TRP/INV-DUP rearrangement followed by isoUPD. Detailed molecular genetic analyses at the sequence level revealed the presence of microhomology at two breakpoint junctions of the CGR, probably underlying the formation of the complicated genomic alteration (CGR + isoUPD). Notably, this is the first case of CGR + isoUPD detected in the long arm of chromosome 1. In addition, the pattern of flanking duplications experimentally documented in the present case, namely, a long duplicated segment with a size on the order of megabases at the centromeric junction observed by CMA with a short duplication at the telomeric junction only identified by sequencing of the breakpoint, has not been reported previously.

Case presentation

The 25-year-old Japanese male reported on here was the first child of a non-consanguineous healthy mother (G0P0, 24 years of age) and father (details are unclear due to a divorce) with no notable family disease history. After an uncomplicated pregnancy, he had been born at 38 weeks of gestation by a normal delivery. His birth weight was 1958 g (−2.52 SD) and he was introduced into a neonatal incubator to treat intrauterine growth

retardation (IUGR) and poor sucking by tube feeding for 20 days, although detailed medical records of his physique are not available. Physical examination at the age of 1 month showed height 46 cm (−3.4 SD), weight 2715 g (−2.6 SD), and head circumference 29.8 cm (−4.6 SD). The abilities to hold up his head, eat solid food, imitate the behaviors of others, and walk alone were recognized at 6 months, 18 months, 2 years and 6 months, and 3 years of age, respectively. The patient had never been able to speak until now, and his comprehension was limited to simple signs, but he recognized various sounds. At 3 years of age, he was diagnosed with the congenital heart defect of tetralogy of Fallot (TOF) but was not treated surgically, although he showed frequent squatting and cyanotic attacks. On physical examination at 24 years and 6 months of age, he showed growth retardation with height 136 cm (−6 SD), weight 28.1 kg (−3.3 SD), and severe mental retardation with a developmental quotient of 5. At 25 years of age, he had TOF, bilateral congenital inguinal hernia, bilateral cryptorchidism, club feet, scoliosis, Chilaiditi's syndrome, and several facial anomalies, such as thinning of the hair, strabismus, widely spaced eyes, a down-slanted palpebral fissure, low-set ears, a prominent forehead, and a coarse face. He has some missing teeth due to having suffered from periodontal disease. Serial complete blood counts showed thrombocytopenia, and magnetic resonance imaging showed cerebral atrophy especially of the frontal lobe, with enlargement of the ventricles. His karyotype at birth was reported to be normal, but repeatedly performed karyotyping revealed 46,XY,dup(1)(q32.1q42.1),inv(9)(p12q13).

Molecular cytogenetic studies

This research protocol for this study was approved by the local ethics committee of Tokushima University. Written informed consent for the participation of the patient in this study was obtained from the patient's mother DNA was extracted from a peripheral blood sample.

A high-resolution CMA using the CytoScan HD array (Affymetrix, Santa Clara, CA) with Chromosome Analysis Suite software (ChAS, Affymetrix) to process the raw data detected a 9.2-Mb trisomy at 1q42.12-q42.2, a 6.7-Mb tetrasomy consisting of the duplication of two haplotypes, each of which probably derives from either the father or the mother, at 1q42.2-q43, and a 8.2-Mb segment with the absence of heterozygosity at 1q43-qter consistent with isoUPD (arr[hg19]1q42.12q42.2(225,101,799_234,324,222)x3,1q42.2q43(234,330,738_240,992,219)x4,1q43qter(240,993,835_249,224,684)x2 hmz, Fig. 1a). Trisomic, tetrasomic, and iUPD regions contain 88, 38, and 94 Refseq genes, and 49, 21, and 24 OMIM genes, respectively. Neither copy number abnormalities nor iUPD around 1q42.2-qter was detected in the DNA of the patient's mother (data not shown). Since the genotyping

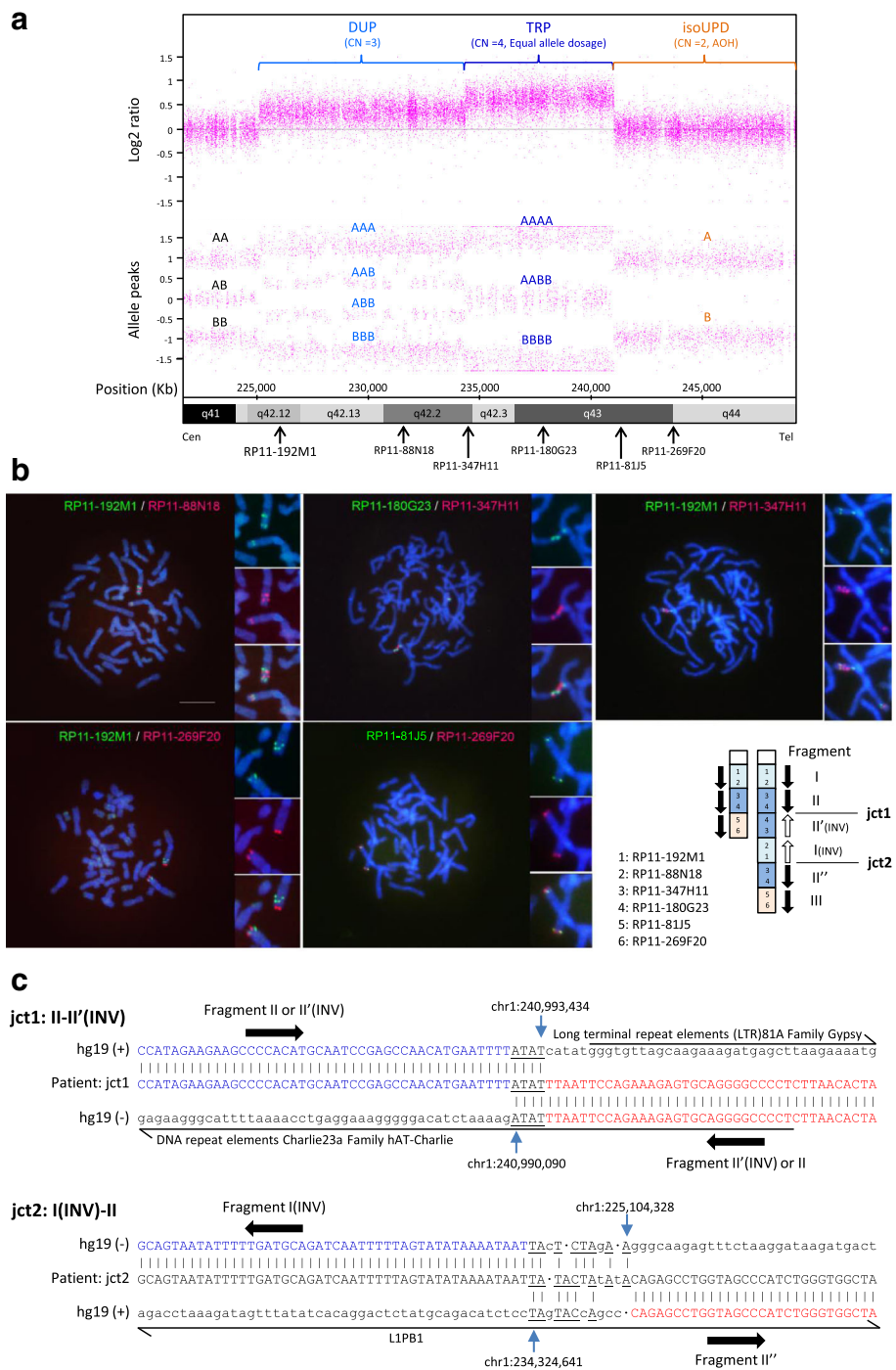


Fig. 1 (See legend on next page.)

(See figure on previous page.)

Fig. 1 a Chromosome Analysis Suite (ChAS) graphic results of Affymetrix CytoScan HD analysis for the 1q region that presented duplication (DUP), triplication (TRP), or isoUPD in the patient. Detection of CGR and isoUPD were performed using an Affymetrix CytoScan HD CMA platform (Affymetrix), which provides 906,600 polymorphic (SNP) and 946,000 non-polymorphic (CNV) markers, according to the manufacturer's recommendations. In addition, we used Chromosome Analysis Suite software (ChAS, Affymetrix) to process the raw data, and the output data were interpreted with the UCSC Genome Browser (<http://genome.ucsc.edu>; GRCh37/hg19 assembly). *Top*, copy number log₂ ratio; *bottom*, allele peaks. CN, copy number. Possible genotype calls based on the allele dosage normalization algorithm are shown using A and B. The location of each BAC used for FISH analysis is shown. **b** Images of two-color FISH mapping using six BAC clones and the scheme of distal 1q CGR based on FISH data. Metaphase FISH images with high-magnification images of the distal 1q. BAC clones labeled with either FITC (*green*) or rhodamine (*red*) were hybridized to 4',6-diamidino-2-phenylindole (DAPI)-stained chromosomes of the patient. The location and detailed information of each BAC are shown in Fig. 1a and Additional file 1: Table S1, respectively. In the scheme, arrows indicate the direction of chromosomal fragments I, II (II', II''), and III, which presented duplication, triplication, and isoUPD, respectively, in CMA. Two junctions (jct 1 and jct2) between fragments II and II' and between I and II'' are also shown. **c** Color-matched sequence alignment of breakpoint junctions in rearrangements. *Top*, jct1 (breakpoint junction 1 between segments II and II'); *bottom*, jct2 (breakpoint junction 2 between segments I and II'') (see Fig. 1b). Microhomology at the junctions is represented by underlined letters. Frequent mismatch sequences were only observed near jct2 within long-range PCR products (data not shown). Thick arrows indicate the possible orientation of chromosomal fragments. Various types of repeat elements observed around junctions are shown

results using SNP typing probe within the iUPD region of the patient matched at least one of the maternal alleles, the iUPD segment is likely to have been inherited from his mother (data not shown), although genomic DNA of his father was not available to confirm the inheritance of this region. On the other hand, genotyping results within the trisomic region suggest that the duplicated segment is unlikely to have been inherited from his mother (data not shown). In the tetrasomic region (the triplicated segment), three allele peaks (AA, AB, and BB) with unusually large spaces between them were observed (Fig. 1a), suggesting the presence of AA/AA, AA/BB, and BB/BB tracks, which is only possible if each parent contributed equally with two alleles (either AA or BB).

Next, the location and orientation of each segment within this structurally altered region were determined by a series of dual-color fluorescence *in situ* hybridization (FISH) studies using bacterial artificial chromosome (BAC) clones located around the region (Fig. 1a and b, Additional file 1: Table S1) performed as described elsewhere [9]. Two signals (duplication) with a direct-inverted orientation and three signals (triplication) with a direct-inverted-direct orientation were detected by probes on the trisomic and tetrasomic regions, respectively. The triplicated segment in an inverted orientation was observed between the proximal triplicated segment in a direct orientation (junction 1, jct1) and the distal duplicated segment in an inverse orientation. The distal triplicated segment in a direct orientation is joined with the inversely oriented distal duplicated segment (junction 2, jct2). The isoUPD segment is then joined with this triplicated segment and terminates the abnormal chromosome 1. Taking these findings together, the final karyotype was interpreted as 46,XY,der(1)dup trp(pter → q43::q43 → q42.12::q42.2 → qter).

Genomic investigation

For the precise mapping of breakpoint junctions in the CGR (jct 1 and 2), we first performed mate pair next-

generation sequencing using the Nextera Mate Pair Sample Preparation Kit and Illumina HiSeq 1500 with 100 paired-end cycles according to the manufacturer instructions (Illumina, San Diego, CA). Reads were aligned to the human genome sequence using the Burrows-Wheeler Alignment tool 0.7.12. (<http://bio-bwa.sourceforge.net>). Two recurrent structural variations within 1q42.12-1qter were identified from the discordant read pairs around the estimated boundary areas by the expected number of reads per region and visual inspection using the Integrative Genomics Viewer. Long-range polymerase chain reaction (PCR) using primers designed around the estimated boundaries (Additional file 2: Table S2) and Takara LA Taq (Takara Bio, Otsu, Japan) with the two step protocol according to the manufacturer instructions. The direct sequencing of PCR products defined sequences around two breakpoint junctions, jct1 and jct2 (Fig. 1c). Based on these results, the duplication and the triplication start around chr1:225,104,328 and 234,324,641, respectively, and the triplication stops around 240,990,090. Interestingly, the small telomeric duplication, namely, of approximately 3 Kb, which evaded CMA detection, is located between 240,990,090 and 240,993,434, and isoUPD starts around 240,993,434, although the copy number of the distal flanking duplication was not experimentally validated. Therefore, the CGR observed in our case seems to involve triplication with flanking duplications, which has been characterized as a type II triplication proposed by Liu et al. [10] with a particular DUP-TRP/INV-DUP structure, and isoUPD was also reported to be associated with this type of CGR [5]. Notably, all reported cases with triplication with flanking duplications followed by isoUPD have small flanking duplications (<0.258 Mb and <0.004 Mb in proximal and distal duplications, respectively) [5], indicating that our case is the first with a large proximal duplication (approximately 9.2 Mb) in this type of CGR. Microhomology (ATAT) was observed at the jct1 breakpoint interval, whereas a microhomologous sequence with some mismatch sequences including insertions, deletion,

and point mutations was observed at the jct2 breakpoint interval (Fig. 1c). Mismatch sequences only near jct2 of CGR, which might occur during the same event as the *de novo* CGR/isoUPD formation, have previously been reported [5]. These mismatch sequences near to the breakpoint junctions of CGR are proposed to be one of the potential signature features of highly error prone replication-based mechanisms using DNA polymerase(s) of low fidelity or a replisome with reduced fidelity [2], although it remains unclear why mismatch sequences have been observed only in jct2 of CGR/isoUPD cases.

Within the isoUPD region, three genes were associated with four autosomal recessive diseases, as determined by a search of the Online Mendelian Inheritance in Man database (OMIM, <http://www.omim.org>, accessed 1 December, 2016; Additional file 3: Table S3). No phenotypes matching these four diseases were observed in the patient described here, and no pathogenic mutation was found in the three genes by Sanger sequencing. In addition, databases of imprinted genes, such as Geneimprint (<http://www.geneimprint.com/site/genes-by-species>, accessed 1 December, 2016) and the Catalogue of Parent of Origin Effects (<http://igc.otago.ac.nz/home.html>, accessed 1 December, 2016), indicated that there are no known imprinting genes within this isoUPD region.

Discussion

In the case presented here, our comprehensive analyses of all of the cytogenetic, microarray, and sequencing data suggest that the MMBIR-based template-switching model (Fig. 2a) recently proposed by Carvalho et al. [5] is one of the most plausible mechanisms underlying the gain of interstitial copy number followed by distal isoUPD to the telomere, which has not previously been described in the long arm of chromosome 1. In this model, two-step template switches triggered by stalled or collapsed replication forks might have occurred. The first template switch is supposed to use a sister chromatid to resume replication. Microhomology at the annealing site (jct1, Fig. 1c) in the complementary strand close to breakpoint is used to prime DNA synthesis, although it is difficult to determine whether this template switching occurred between c and d_c or d and c_c in our sequencing method. Then, unidirectional replication resumes in an inverted orientation and forms an inverted partially duplicated segment. A new event of fork stalling or collapsing might occur and release a free 3' end, which can be resolved by a second template switch to the homologous chromosome using microhomology again, resulting in the formation of a jct2 (Figs. 1c and 2a). This second compensating inversion might contribute to result in a viable cell. A target annealing site was selected between alleles B and C in the present case, and the derivative chromosome results in a DUP-TRP/INV-DUP structure

with a unique long proximal duplicated region (b and b_c , Fig. 2b). Because BIR cannot account for the observations of microhomology identified in both jct1 and jct2 (Fig. 1c), MMBIR is probably involved in resolving both the first and the second breaks. In our case and some previously reported cases [5], however, various mismatch sequences including insertions, deletions, and/or point mutations around breakpoint junction sequences were observed only in jct2 of CGR and the size of the proximal duplicated region containing jct2 was commonly larger than that of the distal duplicated region containing jct1. Therefore, the accomplishment of the resolution of the second break might need additional mechanisms. It also remains unknown whether those two events occurred either all at once in a post-zygotic mitotic cell or in two steps: the first step occurring in a pre-meiotic cell was resolved by the second step occurring in a post-zygotic cell. These alternatives cannot be distinguished using the current data. In addition, it is also difficult to rule out tissue-specific mosaicism as a post-fertilization mitotic event in this case, although no finding of mosaicism was observed in all data obtained from the peripheral leukocytes/lymphocytes of the patient.

Recently, several cases along with our own with concurrent triplication (tetrasomy) and isoUPD, which may be explained by the MMBIR-based mechanism, detected by CMA containing SNP probes, have been reported [4–7]. However, detailed analyses of centromeric and telomeric junctions of triplicated regions in a tiling array or at the sequence level have only been performed on the cases reported by Carvalho et al. [5] and the present case. In most of those cases with detailed junctional analyses, relatively short flanking duplications were observed. These findings suggest that the small size of flanking duplications might have led to the evasion of array-based detection in three reported cases without detailed junction analyses [4, 6, 7]. Indeed, the concurrent triplication (tetrasomy) and isoUPD were detected by Affymetrix arrays including SNP probes in all cases, but a flanking duplication was observed in this analysis only at the centromeric junction in the present case. In addition, microhomology was observed in breakpoint junctions in most of the cases with the DUP-TRP/INV-DUP rearrangement followed by isoUPD reported by Carvalho et al. [5] and the present case, suggesting that an MMBIR-based mechanism might underline the formation of at least this type of genomic alteration implicated in constitutional disorders. Detailed junction analyses of additional cases showing CGRs + isoUPD will be needed to provide support for an MMBIR-based mechanism inducing complex copy number gains and segmental isoUPD in tandem in subjects with multiple congenital anomalies.

Because partial 1q trisomy is a rare disorder and unbalanced chromosomal translocations are often observed

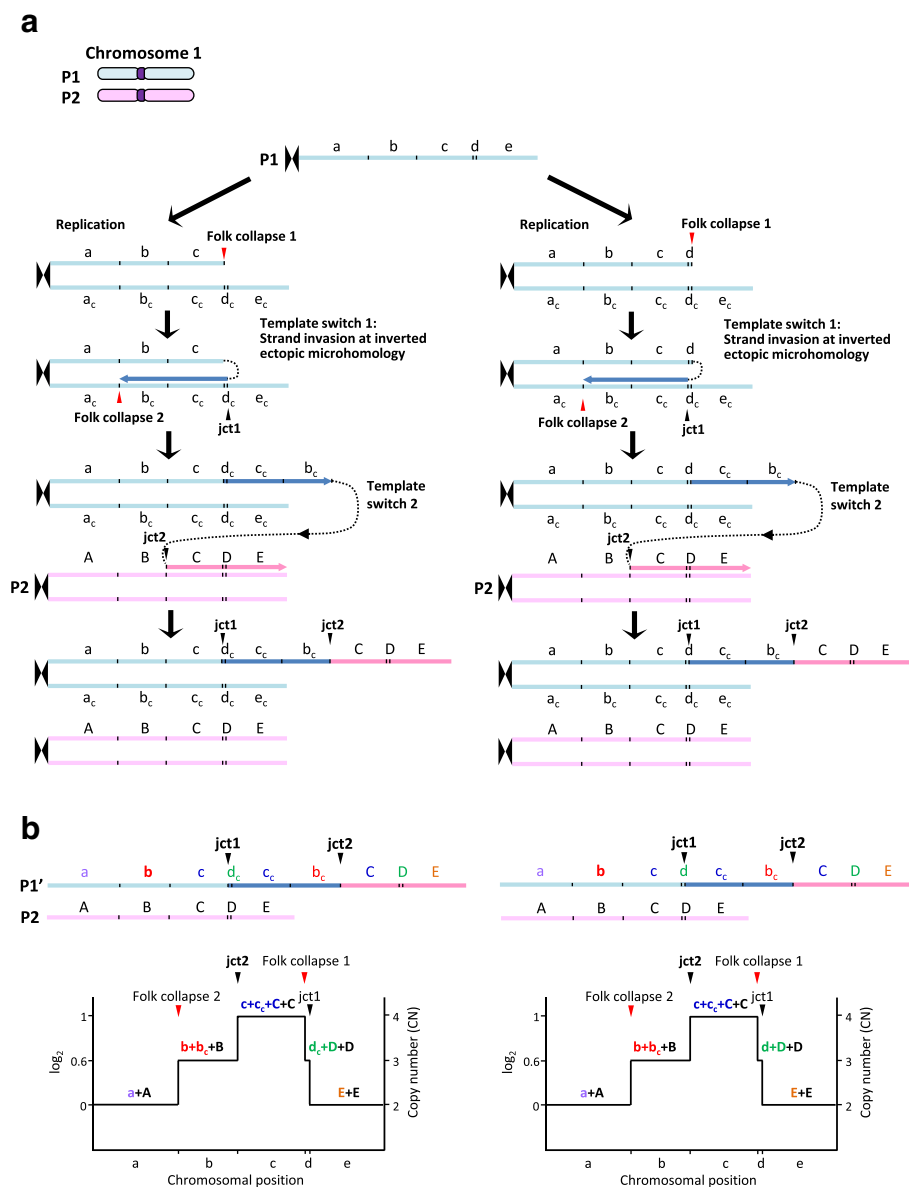


Fig. 2 Replication-based mechanism model for the generation of DUP-TRP/INV-DUP rearrangement followed by isoUPD detected in the present case. **a** The event probably occurred involving parental homolog chromosomes, P1 and P2. The first template switch (template switch 1) have been triggered by a stalled or collapsed replication fork (fork collapse 1), and used a complementary strand to resume replication through using microhomology in the complementary strand at the annealing site (jct1, Fig. 1c) to prime DNA synthesis, resulting in the production of a segment with the inverse orientation compared with the reference genome. Two putative jct1 sites, jct1 between c and d_c (left) and jct1 between d and d_c (right) are predicted, because the same sequence result can be obtained in both cases (see Fig. 1c). Then, a new fork stalling or collapsing event (fork collapse 2) have released a free 3' end that can be resolved by the second template switching (template switch 2) through using the microhomology in the homologous chromosome at the annealing site (jct2, Fig. 1c) to prime and resume DNA synthesis, resulting in the generation of jct2 as well as isoUPD. a–d, representative chromosome alleles in P1 chromosome; a_c–e_c, complementary chromosome alleles in P1 chromosome; A–E: corresponding homologous chromosome alleles in the P2 chromosome. **b** *Top*: different genomic structures are predicted to be generated depending on the location of the selected annealing site (jct1) to prime DNA synthesis in the first template switch event. isoUPD will result if the unidirectional replication fork continues until the telomere. *Bottom*: predicted segmental CNV in a simulated CMA. Note that the small size of the telomeric duplication between fork collapse 1 and jct1 led to the evasion of CMA detection (Fig. 1a), because the region was too small to be detected by Affymetrix Cytoscan HD array

with this alteration [11–16], it is difficult to evaluate the contribution of 1q trisomy to the phenotype in cases involving another chromosome. Patients with pure

partial distal trisomy 1q are known to demonstrate a wide range of manifestations of variable severity. However, distal 1q duplication syndrome is characterized by the

signs present in many of the previously reported cases [15, 16]. The present case showed some of the symptoms characteristic of distal 1q duplication syndrome, such as psychomotor developmental delay, cardiac defect, widely spaced eyes, a down-slanted palpebral fissure, low-set ear, a prominent forehead, club feet, and scoliosis, although psychomotor developmental delay and cardiac defect were very severe compared with those in previously reported cases and some features commonly found elsewhere were not observed [15, 16]. Because the present patient is the first known case of pure distal partial 1q tetrasomy and trisomy, it is possible that the copy number increase in some of the genes located between 1q42.12 and the middle of 1q43 (approximately 180 RefSeq genes) contributes to these symptoms, although no causal regions responsible for each symptom of distal trisomy/tetrasomy 1 syndrome have been clarified. In addition, the influence of isoUPD on the clinical features of the present case remains unknown because of a lack of reported cases with distal 1q UPD.

Conclusions

We report the first case with concurrent CGR (duplications and triplication) + isoUPD in 1q42.12-qter, from an initial diagnosis of interstitial trisomy 1q by conventional karyotyping. Comprehensive cytogenetic and molecular analyses provide additional evidence that DUP-TRP/INV-DUP rearrangement having a unique long proximal DUP structure followed by isoUPD may be generated by an MMBIR-based mechanism. Because it is almost impossible to quantify precise chromosomal copy numbers and detect UPD by conventional karyotyping, molecular cytogenetic analyses using CMA containing SNP probes with additional detailed analyses of the breakpoint junctions in a sequence level are recommended in cases suspected of having complex chromosomal abnormalities based on clinical and cytogenetic findings.

Additional files

Additional file 1: Table S1. BAC clones used in FISH experiments. (DOCX 14 kb)

Additional file 2: Table S2. List of primer sets used in PCR and sequencing for junctions of the CGR. (DOCX 14 kb)

Additional file 3: Table S3. Autosomal recessive diseases and causative genes around the isoUPD region. (DOCX 14 kb)

Abbreviations

BAC: Bacterial artificial chromosome; CGR: Complex genomic rearrangements; CMA: Chromosomal microarray; CNV: Copy number variation; DUP-TRP/INV-DUP: Duplication-inverted triplication-duplication; FISH: Fluorescence *in situ* hybridization; isoUPD: Uniparental isodisomy; IUGR: Intrauterine growth retardation; MCA: Multiple congenital anomalies; MMBIR: Microhomology-mediated break-induced replication; PCR: Polymerase chain reaction; SNP: Single-nucleotide polymorphism; TOF: Tetralogy of Fallot

Acknowledgements

We thank the patient and his mother for their participation in this study and the Support Center for Advanced Medical Sciences, Graduate School of Biomedical Sciences, Tokushima University for technical assistances. This work was partly performed in the Cooperative Research Project Program of the Medical Institute of Bioregulation, Kyushu University.

Funding

This study was supported by JSPS KAKENHI Grant Numbers 26293304, 16K15618, and 15K19620 from the Ministry of Education, Culture, Sports, Science and Technology, Japan, and there is no role for funding agent in this study.

Availability of data and materials

The datasets supporting the conclusions of this article are included within the article and its additional file. More details are available on request.

Authors' contributions

TK, NO, and TN performed the genetic analysis and drafted the paper. CM performed the FISH experiments. YO, NF, and HI performed the genetic analysis. SS and NO collected the data of the patient. MS, KM, and HK contributed in writing the manuscript. II performed CMA, contributed in writing the manuscript, and supervised the study. All the authors have read and approved the final manuscript.

Competing interests

The authors declare that they have no competing interests.

Consent for publication

Mother of the patient has given her informed written consent for publication of the present case report.

Ethics approval and consent to participate

The research protocol for this study was approved by the local ethics committee of Tokushima University. Written informed consent for the participation of the patient in this study was obtained from the patient's mother.

Publisher's Note

Springer Nature remains neutral with regard to jurisdictional claims in published maps and institutional affiliations.

Author details

¹Department of Human Genetics, Graduate School of Biomedical Sciences, Tokushima University, 3-18-15 Kuramoto-cho, Tokushima 770-8503, Japan. ²Department of Oral and Maxillofacial Surgery, Kobe University Graduate School of Medicine, 7-5-1 Kusunoki-cho, Chuo-ku, Kobe, Hyogo 650-0017, Japan. ³Division of Molecular Genetics, Institute for Comprehensive Medical Science, Fujita Health University, 1-98 Dengakugakubo Kutsukake-cho, Toyoake, Aichi 470-1192, Japan. ⁴Japanese Red Cross Tokushima Hinomine Rehabilitation Center for People with Disabilities, 4-1 Shinkai Chuden-cho, Komatsushima, Tokushima 773-0015, Japan. ⁵Department of Medical Genetics, Osaka Medical Center and Research Institute for Maternal and Child Health, 840 Murodo-cho, Izumi, Osaka 594-1101, Japan.

Received: 15 March 2017 Accepted: 21 April 2017

Published online: 28 April 2017

References

- Zhang F, Carvalho CM, Lupski JR. Complex human chromosomal and genomic rearrangements. *Trends Genet.* 2009;25:298–307.
- Carvalho CM, Pehlivan D, Ramocki MB, Fang P, Alleva B, Franco LM, et al. Replicative mechanisms for CNV formation are error prone. *Nat Genet.* 2013;45:1319–26.
- Beneteau C, Landais E, Doco-Fenzy M, Gavazzi C, Philippe C, Béri-Dexheimer M, et al. Microtriplication of 11q24.1: a highly recognisable phenotype with short stature, distinctive facial features, keratoconus, overweight, and intellectual disability. *J Med Genet.* 2011;48:635–9.
- Fujita A, Suzumura H, Nakashima M, Tsurusaki Y, Saito H, Harada N, et al. A unique case of de novo 5q33.3-q34 triplication with uniparental isodisomy of 5q34-qter. *Am J Med Genet A.* 2013;161A:1904–9.

5. Carvalho CM, Pfundt R, King DA, Lindsay SJ, Zuccherato LW, Macville MV, et al. Absence of heterozygosity due to template switching during replicative rearrangements. *Am J Hum Genet.* 2015;96:555–64.
6. Sahoo T, Wang JC, Elnaggar MM, Sanchez-Lara P, Ross LP, Mahon LW, et al. Concurrent triplication and uniparental isodisomy: evidence for microhomology-mediated break-induced replication model for genomic rearrangements. *Eur J Hum Genet.* 2015;23:61–6.
7. Xiao B, Xu H, Ye H, Hu Q, Chen Y, Qiu W. De novo 11q13.4q14.3 tetrasomy with uniparental isodisomy for 11q14.3qter. *Am J Med Genet A.* 2015;167A:2327–33.
8. Wiszniewska J, Bi W, Shaw C, Stankiewicz P, Kang SH, Pursley AN, et al. Combined array CGH plus SNP genome analyses in a single assay for optimized clinical testing. *Eur J Hum Genet.* 2014;22:79–87.
9. Murata C, Kuroki Y, Imoto I, Tsukahara M, Ikejiri N, Kuroiwa A. Initiation of recombination suppression and PAR formation during the early stages of neo-sex chromosome differentiation in the Okinawa spiny rat, *Tokudaia muenninki*. *BMC Evol Biol.* 2015;15:234.
10. Liu P, Carvalho CM, Hastings PJ, Lupski JR. Mechanisms for recurrent and complex human genomic rearrangements. *Curr Opin Genet Dev.* 2012;22:211–20.
11. Nowaczyk MJ, Bayani J, Freeman V, Watts J, Squire J, Xu J. De novo 1q32q44 duplication and distal 1q trisomy syndrome. *Am J Med Genet A.* 2003;120A:229–33.
12. Coccé MC, Villa O, Obregon MG, Salido M, Barreiro C, Solé F, Gallego MS. Duplication dup(1)(q41q44) defined by fluorescence in situ hybridization: delineation of the 'trisomy 1q42- > qter syndrome'. *Cytogenet Genome Res.* 2007;118:84–6.
13. Kulikowski LD, Bellucco FT, Nogueira SI, Christofolini DM, Smith Mde A, de Mello CB, et al. Pure duplication 1q41-qter: further delineation of trisomy 1q syndromes. *Am J Med Genet A.* 2008;146A:2663–7.
14. Balasubramanian M, Barber JC, Collinson MN, Huang S, Maloney VK, Bunyan D, Foulds N. Inverted duplication of 1q32.1 to 1q44 characterized by array CGH and review of distal 1q partial trisomy. *Am J Med Genet A.* 2009;149A:793–7.
15. Watanabe S, Shimizu K, Ohashi H, Kosaki R, Okamoto N, Shimojima K, et al. Detailed analysis of 26 cases of 1q partial duplication/triplication syndrome. *Am J Med Genet A.* 2016;170A:908–17.
16. Morris ML, Baroneza JE, Teixeira P, Medina CT, Cordoba MS, Versiani BR, Roese LL, Freitas EL, Fonseca AC, Dos Santos MC, Pic-Taylor A, Rosenberg C, Oliveira SF, Ferrari I, Mazzeu JF. Partial 1q duplications and associated phenotype. *Mol Syndromol.* 2016;6:297–303.

Submit your next manuscript to BioMed Central and we will help you at every step:

- We accept pre-submission inquiries
- Our selector tool helps you to find the most relevant journal
- We provide round the clock customer support
- Convenient online submission
- Thorough peer review
- Inclusion in PubMed and all major indexing services
- Maximum visibility for your research

Submit your manuscript at
www.biomedcentral.com/submit



Complex X-Chromosomal Rearrangements in Two Women with Ovarian Dysfunction: Implications of Chromothripsis/Chromoaniasynthesis-Dependent and -Independent Origins of Complex Genomic Alterations

Erina Suzuki^a Hirohito Shima^a Machiko Toki^b Kunihiko Hanew^c
Keiko Matsubara^a Hiroki Kurahashi^d Satoshi Narumi^a Tsutomu Ogata^{a,e}
Tsutomu Kamimaki^{b,f} Maki Fukami^a

^aDepartment of Molecular Endocrinology, National Research Institute for Child Health and Development, Tokyo, ^bDepartment of Pediatrics, Hiratsuka City Hospital, Hiratsuka, ^cHanew Endocrine Clinic, Sendai, ^dDivision of Molecular Genetics, Institute for Comprehensive Medical Science, Fujita Health University, Toyoake, ^eDepartment of Pediatrics, Hamamatsu University School of Medicine, Hamamatsu, and ^fDepartment of Pediatrics, Shizuoka City Shimizu Hospital, Shizuoka, Japan

Keywords

Chromothripsis · Genomic rearrangement · Isochromosome · Turner syndrome · X inactivation

Abstract

Our current understanding of the phenotypic consequences and the molecular basis of germline complex chromosomal rearrangements remains fragmentary. Here, we report the clinical and molecular characteristics of 2 women with germline complex X-chromosomal rearrangements. Patient 1 presented with nonsyndromic ovarian dysfunction and hyperthyroidism; patient 2 exhibited various Turner syndrome-associated symptoms including ovarian dysfunction, short stature, and autoimmune hypothyroidism. The genomic abnormalities of the patients were characterized by array-based comparative genomic hybridization, high-resolution karyotyping, microsatellite genotyping, X-inactivation anal-

ysis, and bisulfite sequencing. Patient 1 carried a rearrangement of unknown parental origin with a 46,X,der(X)(pter→p22.1::p11.23→q24::q21.3→q24::p11.4→pter) karyotype, indicative of a catastrophic chromosomal reconstruction due to chromothripsis/chromoaniasynthesis. Patient 2 had a paternally derived isochromosome with a 46,X,der(X)(pter→p22.31::q22.1→q10::q10→q22.1::p22.31→pter) karyotype, which likely resulted from 2 independent, sequential events. Both patients showed completely skewed X inactivation. CpG sites at Xp22.3 were hypermethylated in patient 2. The results indicate that germline complex X-chromosomal rearrangements underlie nonsyndromic ovarian dysfunction and Turner syndrome. Disease-causative mechanisms of these rearrangements likely include aberrant DNA methylation, in addition to X-chromosomal mispairing and haplo-

E.S., H.S., and M.T. contributed equally to this study.

insufficiency of genes escaping X inactivation. Notably, our data imply that germline complex X-chromosomal rearrangements are created through both chromothripsis/chromoanasythesis-dependent and -independent processes.

© 2017 S. Karger AG, Basel

Complex chromosomal rearrangements are common in cancer genomes and can also appear in the germline [Liu et al., 2011; Kloosterman and Cuppen, 2013]. To date, germline complex rearrangements have been identified in a small number of individuals [Liu et al., 2011; Ochalski et al., 2011; Auger et al., 2013; Kloosterman and Cuppen, 2013; Plaisancié et al., 2014]. Of these, complex autosomal rearrangements were often associated with congenital malformations and mental retardation, which probably reflect dysfunction or dysregulation of multiple genes on the affected chromosome [Liu et al., 2011; Kloosterman and Cuppen, 2013; Plaisancié et al., 2014]. In contrast, complex X-chromosomal rearrangements were detected primarily in women with nonsyndromic ovarian dysfunction and were occasionally associated with other clinical features such as short stature, muscular hypotonia, and an unmasked X-linked recessive disorder [Ochalski et al., 2011; Auger et al., 2013]. The lack of severe developmental defects in women with complex X-chromosomal rearrangements is consistent with prior observations that structurally abnormal X chromosomes, except for X;autosome translocations, frequently undergo selective X inactivation [Heard et al., 1997]. The clinical features of these women, such as ovarian dysfunction and short stature, are ascribable to X-chromosomal mispairing and haploinsufficiency of genes that escape X inactivation [Zhong and Layman, 2012]. Mutations in *BMP15* at Xp11.22, *POF1B* at Xq21.1, *DIAPH2* at Xq21.33, or *PGRMC1* at Xq24 have been shown to lead to ovarian dysfunction, while mutations in *SHOX* at Xp22.33 impair skeletal growth [Bione et al., 1998; Bione and Toniolo, 2000; Mansouri et al., 2008; Zhong and Layman, 2012]. However, considering the limited number of reported cases, further studies are necessary to clarify the phenotypic characteristics of germline complex X-chromosomal rearrangements. Furthermore, it remains uncertain whether such rearrangements perturb DNA methylation of the affected X chromosomes.

Recent studies revealed that complex genomic rearrangements are caused by catastrophic cellular events referred to as chromothripsis and chromoanasythesis [Liu et al., 2011; Pellestor, 2014; Leibowitz et al., 2015; Zhang et al., 2015]. Chromothripsis is characterized by massive

DNA breaks in a single or a few chromosomes followed by random reassembly of the DNA fragments [Liu et al., 2011; Pellestor, 2014; Zhang et al., 2015]. Chromothripsis is predicted to arise from micronucleus-mediated DNA breakage of mis-segregated chromosomes, although several other mechanisms such as telomere erosion, p53 inactivation, and abortive apoptosis have also been implicated [Liu et al., 2011; Pellestor, 2014; Zhang et al., 2015]. Chromothripsis typically results in copy-number-neutral translocations/inversions or rearrangements with copy number loss; however, in some cases, genomic rearrangements with copy number gain have also been linked to chromothripsis [Liu et al., 2011; Pellestor, 2014]. Copy number gains in these cases are ascribed to replication-based errors during chromosomal reassembly [Liu et al., 2011]. Chromoanasythesis is proposed to arise from serial template switching during DNA replication [Leibowitz et al., 2015]. Chromoanasythesis has been reported as a cause of complex rearrangements with duplications and triplications [Leibowitz et al., 2015]. To date, the clinical significance of germline chromothripsis/chromoanasythesis has not been fully determined. In particular, it remains unknown whether these catastrophic events account for all cases of complex rearrangements in the germline. Here, we report the clinical and molecular characteristics of 2 women with complex X-chromosomal rearrangements.

Patients and Methods

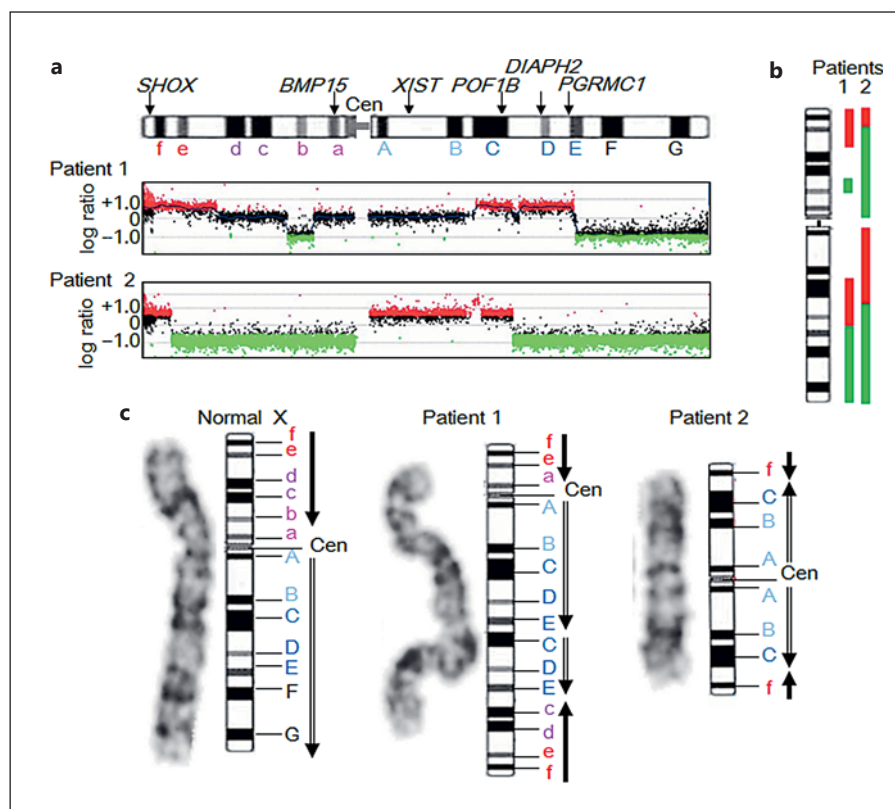
Patients

Patients 1 and 2 were unrelated Japanese women. Patient 1 was hitherto unreported, while patient 2 was previously reported as a female with Turner syndrome [Uehara et al., 2001]. Both patients underwent G-banding analysis in endocrine clinics and were found to have X-chromosomal rearrangements. Thus, they were referred to our institute for further investigation.

Molecular Analysis

Copy number alterations in the genomes were analyzed by comparative genomic hybridization using catalog human arrays (2x400K or 4x180K formats; Agilent Technologies, Palo Alto, CA, USA). We referred to the Database of Genomic Variants (<http://dgv.tcag.ca/dgv/app/home>) to exclude benign copy number polymorphisms. Then, we genotyped 15 microsatellite loci on the X chromosome. Each locus was PCR-amplified using fluorescently labeled forward primers and unlabeled reverse primers. Primer sequences are available from the authors upon request. We also examined the X inactivation status by performing methylation analysis of CpG sites and microsatellite assays of a polymorphic CAG repeat tract in the androgen receptor (*AR*) gene. The methods were described previously [Muroya et al., 1999]. Furthermore, to clarify whether the genomic rearrangements in the patients affect the

Fig. 1. a Array-based comparative genomic hybridization of the patients' X chromosomes. The black, red, and green dots denote normal, increased (log ratio higher than +0.4), and decreased (log ratio lower than -0.8) copy numbers, respectively. The upper panel shows the structure of the X chromosome and the positions of *SHOX*, *BMP15*, *XIST*, *POF1B*, *DIAPH2*, and *PGRMC1*. Cen, centromere. **b** Summary of copy number alterations in patients 1 and 2. The red and green lines depict duplicated and deleted regions, respectively. **c** High-resolution banding of a normal and the rearranged X chromosomes. The black and double-line arrows indicate the orientation of the X chromosome segments (from pter to the centromere and from the centromere to qter, respectively).



DNA methylation of X-chromosomal genes, we performed bisulfite sequencing for CpG sites in the upstream region of *SHOX*. In this experiment, genomic DNA samples were treated with bisulfite using the EZ DNA Methylation Kit (Zymo Research, Irvine, CA, USA). A DNA fragment (chrX:580,597–580,771, hg19, build 37) containing 12 *SHOX*-flanking CpG sites was PCR-amplified using a primer set that hybridizes with both the methylated and unmethylated clones. The PCR products were subcloned with the TOPO TA Cloning Kit (Life Technologies, Carlsbad, CA, USA) and subjected to direct sequencing.

Results

Clinical Manifestations of Patients 1 and 2

Patient 1 was born to phenotypically normal nonconsanguineous parents. This patient showed normal growth during childhood. At 12 years of age, she developed goiter. She was diagnosed with hyperthyroidism and was treated with propylthiouracil for 13 years. This patient exhibited age-appropriate sexual development and experienced menarche at 12 years of age (mean menarcheal age in the Japanese population: 12.3 years). However, her menstrual cycles were irregular and ceased at 15 years of age. Blood examinations at 26 years of age revealed mark-

edly increased gonadotropin levels. She received estrogen and progesterone supplementation and had periodic withdrawal bleeding. She was otherwise healthy and had no Turner stigmata. Her mental development was normal. Her adult height was within the normal range (151.0 cm, -1.3 SD).

Patient 2 was previously reported as a female with Turner syndrome [Uehara et al., 2001]. At 16 years of age, she presented with short neck, shield chest, and cubitus valgus. She also exhibited hypertension, diabetes mellitus, and autoimmune hypothyroidism. In addition, she showed severe short stature (138 cm, -3.8 SD) despite being treated with growth hormone from 8 years of age. She lacked spontaneous pubertal development and was diagnosed with hypogonadism. Her mental development was normal.

Characterization of Genomic Rearrangements

Patient 1 had a 46,X,der(X)(pter→p22.1::p11.23→q24::q21.3→q24::p11.4→pter) karyotype (Fig. 1). The rearranged X chromosome involved at least 5 breakpoints and showed copy number gain of ~20-Mb and ~27-Mb regions at Xp and Xq, respectively, and copy number loss of ~7-Mb and ~36-Mb regions at Xp and Xq, respective-

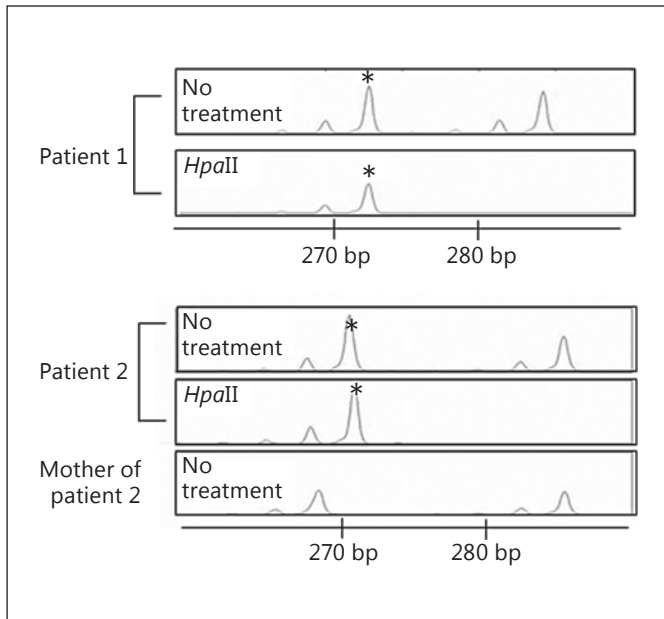


Fig. 2. X-inactivation analysis of *AR*. Microsatellite analysis was performed for polymorphic dinucleotide repeats before and after digestion with the methylation-sensitive enzyme *HpaII*. In patient 1, the 274-bp peak (indicated by an asterisk) represents the PCR products amplified from the inactive X chromosome, while the 283-bp peak indicates the products amplified from the active X chromosome. In patient 2, the 271-bp peak (asterisk) represents the PCR products amplified from the inactive rearranged X chromosome, while the 286-bp peak depicts the products amplified from the maternally transmitted normal X chromosome. These data suggest that the rearranged X chromosome of patient 2 was of paternal origin.

Table 1. Representative results of the microsatellite analysis in patient 2 and her mother

Locus	Chromosomal position ^a	Copy number in the genome of patient 2	PCR products, bp	
			patient 2	mother
<i>SHOX</i> (CA)	Xp22.33	3	142/150	132/142
DXYS233	Xp22.33	3	277	277
DXYS85	Xp22.33	3	200/204	204
DXS1449	Xp22.33	3	116	116
DXS85	Xp22.2	3	174/232	174/232
DXS8025	Xp11.4	1	186	180/186
DXS1069	Xp11.4	1	256	256
DXS1068	Xp11.4	1	254	250/254
<i>ALAS2</i>	Xp11.21	1	155	155/157
<i>AR</i>	Xq12	3	271/286	268/286
DXS8020	Xq22.1	3	194/196	194/196
<i>HPRT1</i>	Xq26.2–26.3	1	290	282/290
DXS8377	Xq28	1	233	229/233
DXS7423	Xq28	1	187	183/187
DXS15	Xq28	1	148	146/148

^a Based on Ensembl Genome Browser (<http://www.ensembl.org>).

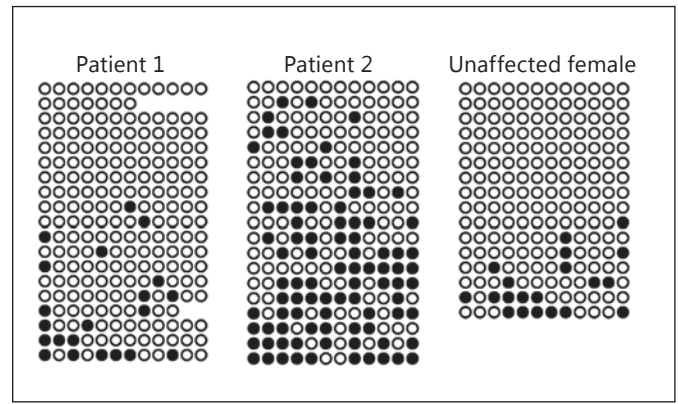


Fig. 3. Methylation analysis of *SHOX*-flanking CpG sites. Each horizontal line indicates the results of 1 clone. Filled and open circles indicate methylated and unmethylated cytosines in the CpG dinucleotides, respectively.

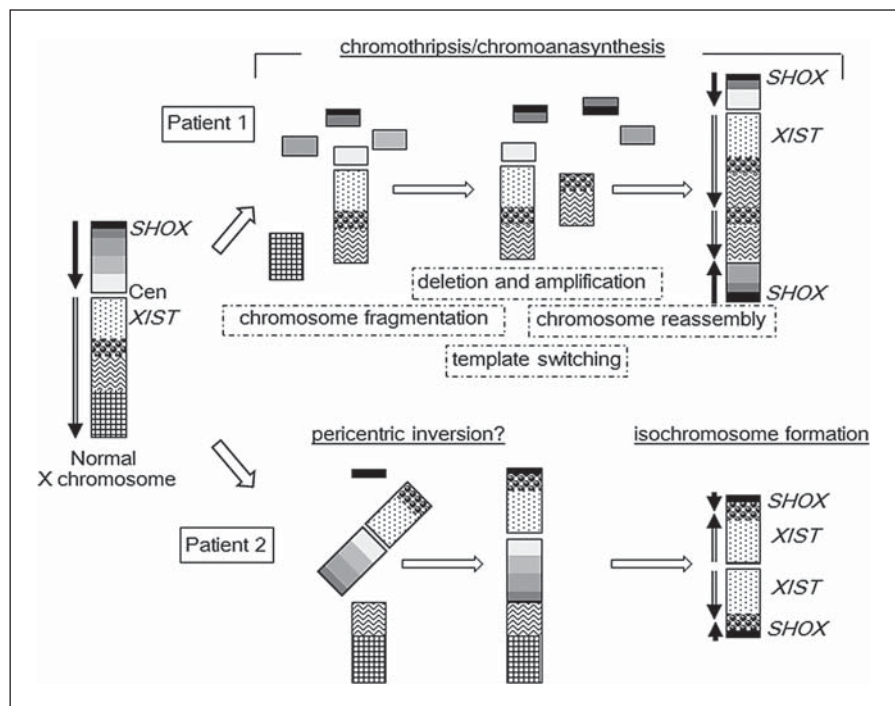
ly. This rearrangement caused overdosage of *SHOX*, *POF1B*, *DIAPH2*, and *PGRMC1* but did not affect the copy number of *BMP15* or *XIST* (X inactive specific transcript). X-inactivation analysis confirmed completely skewed inactivation (Fig. 2). *SHOX*-flanking CpG sites were barely methylated both in patient 1 and in an unaffected control individual (Fig. 3).

Patient 2 had a 46,X,der(X)(pter→p22.31::q22.1→q10::q10→q22.1::p22.31→pter) karyotype (Fig. 1). The rearranged X chromosome comprised at least 3 breakpoints and showed copy number gain of an ~8-Mb region at Xp and an ~40-Mb region at Xq and copy number loss of an ~53-Mb region at Xp and an ~54-Mb region at Xq. *SHOX*, *XIST*, and *POF1B* were duplicated, while *BMP15*, *DIAPH2*, and *PGRMC1* were deleted. There were no copy-number-neutral regions on this X chromosome. Microsatellite analysis suggested that this chromosome consisted of 2 identical arms (“isochromosome”) of paternal origin (Table 1). The rearranged X chromosome was selectively inactivated (Fig. 2). *SHOX*-flanking CpG islands in patient 2 were hypermethylated (Fig. 3).

Discussion

We characterized complex germline X-chromosomal rearrangements in 2 patients. The clinical manifestations of the patients are consistent with the genomic structure. First, both patients manifested ovarian dysfunction. This feature is attributable to X-chromosomal mispairing, as suggested in cases of Turner syndrome due to X mono-

Fig. 4. Predicted mechanisms of the chromosomal rearrangements. The black and double-line arrows indicate the orientation of X chromosome segments (from pter to the centromere and from the centromere to qter, respectively). The rearranged X in patient 1 is consistent with a catastrophic reconstruction due to chromothripsis/chromoanasythesis, while that in patient 2 likely results from 2 independent sequential events. It remains to be clarified whether the father of patient 2 carries a pericentric inversion.



somy [Ogata and Matsuo, 1995]. Furthermore, patient 2 lacked *BMP15*, *DIAPH2*, and *PGRMC1*, which have been implicated in ovarian function [Bione et al., 1998; Bione and Toniolo, 2000; Mansouri et al., 2008]. Copy number changes of other genes might also have contributed to the ovarian dysfunction in patients 1 and 2, because multiple X-chromosomal loci have been linked to this phenotype [Zhong and Layman, 2012]. Second, Turner stigmata such as short neck, shield chest, and cubitus valgus were observed in patient 2 but not in patient 1. These results support the previously proposed notion that a lymphogenic gene responsible for Turner stigmata resides at Xp11.2 [Ogata et al., 2001a], a genomic region deleted in patient 2 and preserved in patient 1. Third, both patients manifested thyroid disorders. Notably, isochromosome Xq is known to be associated with a high risk of autoimmune thyroid disorders [Elsheikh et al., 2001]. Indeed, the hypothyroidism of patient 2 may have resulted from copy number gain of *GPR174* at Xq21.1, because increased expression of *GPR174* has been linked to the risk of an autoimmune thyroid disorder [Chu et al., 2013]. However, the copy number of *GPR174* remained intact in patient 1. Thus, the genomic interval at Xq21.32q22.1>Xq21.32-q22.1, duplicated in both patients, may contain a hitherto uncharacterized gene associated with autoimmune thyroid disorders. Lastly, patient 1 had a normal

stature, and patient 2 showed severe short stature, although both patients carried 3 copies of *SHOX*. This is inconsistent with previous findings that trisomy of the Xp22.3 region encompassing *SHOX* leads to tall stature [Ogata et al., 2001b]. In patients 1 and 2, positive effects of *SHOX* overdosage on skeletal growth may be balanced by negative effects of X-chromosomal mispairing and copy number alterations of minor growth genes on the X chromosome. Furthermore, short stature in patient 2 may be associated with *SHOX* dysregulation, because *SHOX*-flanking CpG islands were hypermethylated in this individual. These sites were barely methylated in the control individual, which is in agreement with the fact that *SHOX* escapes X inactivation [Rao et al., 1997]. It has been shown that in patients with X;autosome translocations, aberrant DNA methylation can spread to regions larger than 1 Mb of the autosomal segments [Cotton et al., 2014]. Hypermethylation of the *SHOX*-flanking CpG sites in patient 2 may reflect decreased physical distance between *SHOX* and *XIST* and/or copy number gain of *XIST*.

The genomic rearrangements in patients 1 and 2 appear to have been formed through different mechanisms (Fig. 4). The rearrangement in patient 1 is consistent with catastrophic reconstruction due to chromothripsis/chromoanasythesis [Liu et al., 2011; Leibowitz et al., 2015].

This case provides further evidence that X-chromosomal chromothripsis/chromoanasythesis accounts for a small portion of cases with nonsyndromic ovarian dysfunction. In contrast, the rearrangement in patient 2 is inconsistent with the “all-at-once” nature of chromothripsis/chromoanasythesis [Liu et al., 2011; Hatch and Hetzer, 2015]. The rearranged chromosome of this patient had 2 identical arms consisting of Xp and Xq material, indicating that this chromosome arose by 2 independent sequential events, namely, a fusion between the Xp22.31 and Xq22.1 segments followed by isochromosome formation. Notably, the rearrangement occurred in the paternally inherited X chromosome. Thus, although the Xp22.31;Xq22.1 translocation is the simplest explanation of this rearrangement, it is implausible in this case, because X;X translocation rarely occurs during male meiosis. The results of patient 2 can be explained by assuming that the phenotypically normal father carried a pericentric inversion, inv(X)(p22.31q22.1), which was subjected to meiotic or postzygotic isochromosome formation (Fig. 4). However, since a paternal DNA sample was not available for genetic testing, we cannot exclude the possibility that this rearrangement was formed via other rare processes.

In conclusion, the results indicate that complex X-chromosomal rearrangements in the germline lead to ovarian dysfunction with and without other Turner syndrome-associated features. Clinical outcomes of such re-

arrangements likely reflect X-chromosomal mispairing, haploinsufficiency of genes escaping X inactivation, and/or perturbed DNA methylation. Most importantly, our findings imply that germline complex X-chromosomal rearrangements are created through both chromothripsis/chromoanasythesis-dependent and -independent processes.

Acknowledgements

This study was supported by the Grants-in-Aid from the Japan Society for the Promotion of Science; and by the Grants from the Ministry of Health, Labor and Welfare, the Japan Agency for Medical Research and Development, the National Center for Child Health and Development, and the Takeda Foundation.

Statement of Ethics

This study was approved by the Institutional Review Board Committee at the National Center for Child Health and Development and performed after obtaining written informed consent.

Disclosure Statement

The authors have no competing interests to declare.

References

- Auger J, Bonnet C, Valduga M, Philippe C, Bertolo-Houriez E, et al: De novo complex X chromosome rearrangement unmasking maternally inherited *CSF2RA* deletion in a girl with pulmonary alveolar proteinosis. *Am J Med Genet A* 161A:2594–2599 (2013).
- Bione S, Toniolo D: X chromosome genes and premature ovarian failure. *Semin Reprod Med* 18:51–57 (2000).
- Bione S, Sala C, Manzini C, Arrigo G, Zuffardi O, et al: A human homologue of the *Drosophila melanogaster diaphanous* gene is disrupted in a patient with premature ovarian failure: evidence for conserved function in oogenesis and implications for human sterility. *Am J Hum Genet* 62:533–541 (1998).
- Chu X, Shen M, Xie F, Miao XJ, Shou WH, et al: An X chromosome-wide association analysis identifies variants in *GPR174* as a risk factor for Graves' disease. *J Med Genet* 50:479–485 (2013).
- Cotton AM, Chen CY, Lam LL, Wasserman WW, Kobor MS, Brown CJ: Spread of X-chromosome inactivation into autosomal sequences: role for DNA elements, chromatin features and chromosomal domains. *Hum Mol Genet* 23:1211–1223 (2014).
- Elsheikh M, Wass JA, Conway GS: Autoimmune thyroid syndrome in women with Turner's syndrome – the association with karyotype. *Clin Endocrinol (Oxf)* 55:223–226 (2001).
- Hatch EM, Hetzer MW: Chromothripsis. *Curr Biol* 25:R397–399 (2015).
- Heard E, Clerc P, Avner P: X-chromosome inactivation in mammals. *Annu Rev Genet* 31:571–610 (1997).
- Kloosterman WP, Cuppen E: Chromothripsis in congenital disorders and cancer: similarities and differences. *Curr Opin Cell Biol* 25:341–348 (2013).
- Leibowitz ML, Zhang CZ, Pellman D: Chromothripsis: A new mechanism for rapid karyotype evolution. *Annu Rev Genet* 49:183–211 (2015).
- Liu P, Erez A, Nagamani SC, Dhar SU, Kołodziejaska KE, et al: Chromosome catastrophes involve replication mechanisms generating complex genomic rearrangements. *Cell* 146:889–903 (2011).
- Mansouri MR, Schuster J, Badhai J, Stattin EL, Lösel R, et al: Alterations in the expression, structure and function of progesterone receptor membrane component-1 (*PGRMC1*) in premature ovarian failure. *Hum Mol Genet* 17:3776–3783 (2008).
- Muroya K, Kosho T, Ogata T, Matsuo M: Female carriers of Xp22.3 deletion including MRX locus. *Am J Med Genet* 84:384–385 (1999).
- Ochalski ME, Engle N, Wakim A, Ravnan BJ, Hoffner L, et al: Complex X chromosome rearrangement delineated by array comparative genome hybridization in a woman with premature ovarian insufficiency. *Fertil Steril* 95:2433.e9–e15 (2011).

- Ogata T, Matsuo N: Turner syndrome and female sex chromosome aberrations: deduction of the principal factors involved in the development of clinical features. *Hum Genet* 95:607–629 (1995).
- Ogata T, Muroya K, Matsuo N, Shinohara O, Yorifuji T, et al: Turner syndrome and Xp deletions: clinical and molecular studies in 47 patients. *J Clin Endocrinol Metab* 86:5498–508 (2001a).
- Ogata T, Matsuo N, Nishimura G: *SHOX* haploinsufficiency and overdosage: impact of gonadal function status. *J Med Genet* 38:1–6 (2001b).
- Pellestor F: Chromothripsis: how does such a catastrophic event impact human reproduction? *Hum Reprod* 29:388–393 (2014).
- Plaisancié J, Kleinfinger P, Cances C, Bazin A, Julia S, et al: Constitutional chromoanapsinthesis: description of a rare chromosomal event in a patient. *Eur J Med Genet* 57:567–570 (2014).
- Rao E, Weiss B, Fukami M, Rump A, Niesler B, et al: Pseudoautosomal deletions encompassing a novel homeobox gene cause growth failure in idiopathic short stature and Turner syndrome. *Nat Genet* 16:54–63 (1997).
- Uehara S, Hanew K, Harada N, Yamamori S, Nata M, et al: Isochromosome consisting of terminal short arm and proximal long arm X in a girl with short stature. *Am J Med Genet* 99:196–199 (2001).
- Zhang CZ, Spektor A, Cornils H, Francis JM, Jackson EK, et al: Chromothripsis from DNA damage in micronuclei. *Nature* 522:179–184 (2015).
- Zhong Q, Layman LC: Genetic considerations in the patient with Turner syndrome – 45,X with or without mosaicism. *Fertil Steril* 98:775–779 (2012).

Intragenic *DOK7* deletion detected by whole-genome sequencing in congenital myasthenic syndromes

OPEN

Yoshiteru Azuma, MD,
PhD
Ana Töpf, PhD
Teresinha Evangelista,
MD
Paulo José Lorenzoni,
MD, PhD
Andreas Roos, PhD
Pedro Viana, MD
Hidehito Inagaki, PhD
Hiroki Kurahashi, MD,
PhD
Hanns Lochmüller, MD

Correspondence to
Dr. Lochmüller:
hanns.lochmuller@newcastle.ac.
uk

ABSTRACT

Objective: To identify the genetic cause in a patient affected by ptosis and exercise-induced muscle weakness and diagnosed with congenital myasthenic syndromes (CMS) using whole-genome sequencing (WGS).

Methods: Candidate gene screening and WGS analysis were performed in the case. Allele-specific PCR was subsequently performed to confirm the copy number variation (CNV) that was suspected from the WGS results.

Results: In addition to the previously reported frameshift mutation c.1124_1127dup, an intragenic 6,261 bp deletion spanning from the 5' untranslated region to intron 2 of the *DOK7* gene was identified by WGS in the patient with CMS. The heterozygous deletion was suspected based on reduced coverage on WGS and confirmed by allele-specific PCR. The breakpoints had microhomology and an inverted repeat, which may have led to the development of the deletion during DNA replication.

Conclusions: We report a CMS case with identification of the breakpoints of the intragenic *DOK7* deletion using WGS analysis. This case illustrates that CNVs undetected by Sanger sequencing may be identified by WGS and highlights their relevance in the molecular diagnosis of a treatable neurologic condition such as CMS. *Neurol Genet* 2017;3:e152; doi: 10.1212/NXG.000000000000152

GLOSSARY

aCGH = array comparative genomic hybridization; **AChE** = acetylcholinesterase; **CMS** = congenital myasthenic syndromes; **CNV** = copy number variation; **MLPA** = multiplex ligation-dependent probe amplification; **MuSK** = muscle-specific tyrosine kinase; **NMJ** = neuromuscular junction; **WES** = whole-exome sequencing; **WGS** = whole-genome sequencing.

Congenital myasthenic syndromes (CMS) are inherited disorders characterized by fatigable muscle weakness with or without other associated signs or symptoms.¹ They are caused by mutations in genes expressed at the neuromuscular junction (NMJ). *DOK7* is one of the components of the NMJ and an activator of the muscle-specific tyrosine kinase (MuSK).² Recessive mutations in *DOK7* cause approximately 10% of the genetically diagnosed CMS cases.¹

CMS are heterogeneous diseases, and to date, more than 25 genes have been reported to be causative. Consecutive single-gene screening has been routinely used as a diagnostic tool; however, next-generation sequencing allows the analysis of all these genes simultaneously to identify the causative variant and obtain a genetic diagnosis. The efficacy of whole-exome sequencing (WES) for the diagnosis of CMS cases has been reported,^{3,4} as well as its ability to identify new causal genes.^{5,6} However, the limitation is that WES is designed to detect only protein-coding regions and exon-intron boundaries of the genome.

Supplemental data
at Neurology.org/ng

From the Institute of Genetic Medicine (Y.A., A.T., T.E., P.J.L., A.R., H.L.), Newcastle University, UK; Division of Neurology (P.J.L.), Federal University of Parana, Brazil; Leibniz-Institut für Analytische Wissenschaften ISAS e.V. (A.R.), Germany; Department of Neurosciences and Mental Health (P.V.), University of Lisbon, Portugal; and Division of Molecular Genetics (H.I., H.K.), Fujita Health University, Japan.

Funding information and disclosures are provided at the end of the article. Go to Neurology.org/ng for full disclosure forms. The Article Processing Charge was funded by the Medical Research Council.

This is an open access article distributed under the terms of the Creative Commons Attribution License 4.0 (CC BY), which permits unrestricted use, distribution, and reproduction in any medium, provided the original work is properly cited.

On the other hand, whole-genome sequencing (WGS) allows the analysis of deep intronic, intergenic, and other noncoding regions. Furthermore, WGS allows to detect copy number variations (CNVs), as coverage is more homogeneous than that of WES.⁷

We present a CMS case in which a large intragenic *DOK7* deletion was identified by WGS compound heterozygous to a known exonic mutation.

METHODS *DOK7* screening. DNA from the patient was extracted from whole blood by standard methods. Screening of hot-spot mutations was performed by Sanger sequencing, encompassing a region of ~600 bp covering the previously reported European founder mutation c.1124_1127dup.² Subsequently, full screening of coding regions and exon-intron boundaries of the *DOK7* gene was performed. Primer sequences are listed in table e-1 at Neurology.org/ng. Annotation of the human *DOK7* cDNA is according to the GenBank accession number NM_173660.

Mutation analysis by WGS. WGS was performed by the TruSeq PCR-free library preparation kit and HiSeqX v2 SBS kit (Illumina, San Diego, CA) for 30× mean coverage on a HiSeqX sequencer. Reads were mapped against hg19 reference genome using the Burrows-Wheeler transform,⁸ and duplicates were removed using Picard tools.⁹

Sequence variants were called using the Genome Analysis Toolkit.¹⁰ WGS data were then analyzed using deCODE's platform (Clinical Sequence Miner; WuXi NextCODE, Cambridge, MA). Rare variants were filtered by threshold of coverage (≥ 8), variant call (≥ 2), and ratio of variant (≥ 0.2) and allele frequency of 1% in 1000 Genomes database.¹¹

Sanger sequencing of large deletion. We amplified DNA samples to identify the suspected intragenic deletion with primers 5'-CCCAGATGGTGCGCTTGCTCC-3' and 5'-GCCACCCCTCACGCTCAG-3'. The PCR protocol comprised 35 cycles and annealing temperature of 68°C using HotStarTaq DNA polymerase with Q-Solution for the GC rich region (QIAGEN, Düsseldorf, Germany).

Standard protocol approvals, registrations, and patient consents. All human studies including genetic analysis were approved by institutional review boards, and appropriate written informed consent was obtained from all the patients and family members.

RESULTS Clinical findings. The patient is a 39-year-old Portuguese man who presented with bilateral ptosis and exercise-induced muscle weakness. He had no family history of muscle disease, and his motor milestones in childhood were normal. He showed mild ptosis from infancy and noticed mild lower limb weakness at 13 years of age. He was admitted to hospital for a month because of sudden severe generalized muscle weakness and worsening ptosis at 15 years of age. He has bilateral facial weakness and winged scapula, and the clinical diagnosis of a neuromuscular transmission defect was confirmed by neurophysiologic studies. EMG showed myopathic

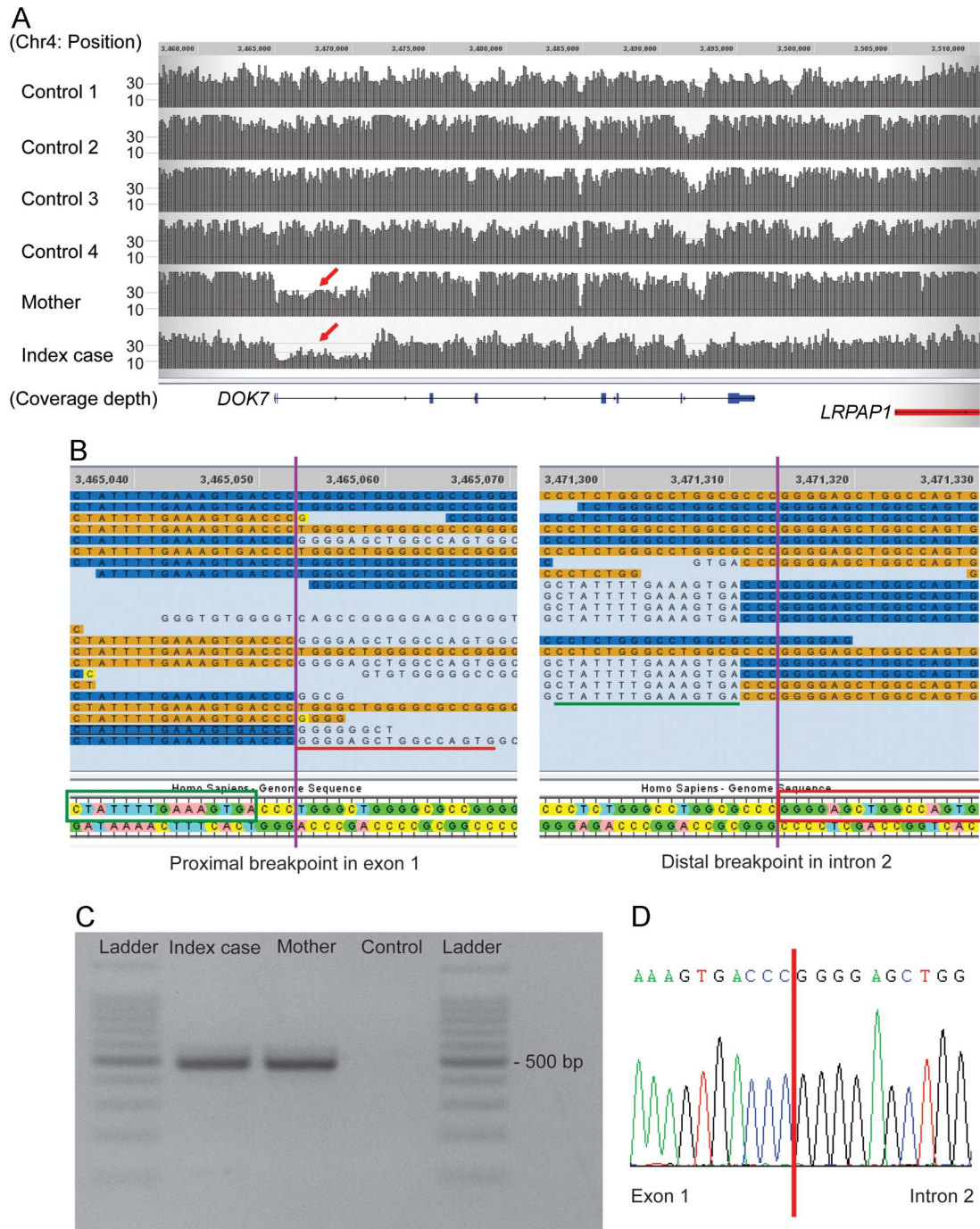
changes on facial muscles. Repetitive nerve stimulation showed a remarkable decremental response of 76% in proximal muscles. Both antiacetylcholine-receptor and anti-MuSK antibodies were negative, and immunosuppressive treatment was unsuccessful. Acetylcholinesterase (AChE) inhibitor of pyridostigmine up to 360 mg/d for 10 years had little effect and was discontinued without clinical deterioration after the trial of oral administration of salbutamol which effected significantly. He has not experienced severe muscle weakness for 5 years since salbutamol was started.

***DOK7* screening.** Based on the limb-girdle clinical presentation of the patient, a hot-spot region of *DOK7* was investigated as a first screening step. Sanger sequencing revealed that the patient carried the heterozygous c.1124_1127dup reported as a founder mutation in European CMS patients.² This mutation was not present in the mother (DNA from the father was unavailable). However, this single heterozygous mutation does not explain *DOK7*-CMS, which invariably shows autosomal recessive inheritance. To identify a second heteroallelic *DOK7* variant, the whole coding region and exon-intron boundaries of the *DOK7* gene were Sanger sequenced, but no potentially pathogenic exonic or splice site variants were found. The sample was therefore subjected to WGS to try to identify other mutations within the *DOK7* gene or elsewhere in the genome.

WGS analysis. As expected, applying a standard pipeline for variant filtering (minor allele frequency 1% in coding region), the heterozygous c.1124_1127dup in *DOK7* was detected in the WGS data. This filtering did not identify any other coding variants in known CMS causal genes.

However, visual inspection of the sequencing reads of the *DOK7* gene for this patient revealed that the read depth for exons 1 and 2 was lower than that of neighboring regions and other control samples (figure 1A). Furthermore, there were no heterozygous variants within this region, indicating a run of homozygosity or hemizyosity suggesting a single copy region. Close inspection of the boundaries of this region showed that in some instances, sections of the sequencing reads did not match the reference sequence. These reads were considered chimeric or split reads, as the unmatched sequences did align to a different region of the genome. Split reads are indicative of structural variation. In fact, the 3' section of the split reads of the proximal boundary aligns to the 3' end of the distal boundary, and vice versa (figure 1B, red underline and red box). The proximal and distal breakpoints lie approximately 6 kb away. These findings suggested that this patient

Figure 1 Whole-genome sequencing analysis and allele-specific PCR



(A) Both index case and his mother show reduced read depth (coverage) from exon 1 to deep intron 2 of the *DOK7* gene (red arrow). Controls 1-4 correspond to samples sequenced and analyzed through the same pipeline and without the diagnosis of congenital myasthenic syndromes. (B) Split reads were observed at both presumed breakpoints. Nucleotides matching the reference sequence of *DOK7* are highlighted in orange/blue. Single unmatched nucleotides are highlighted in yellow, and further unmatched sequences are not highlighted. The unmatched sequence (indicated with red/green underline) of the split reads of the proximal breakpoint aligns to the reference sequence (indicated in green/red boxes) at the distal breakpoint, and vice versa. (C) The expected products amplified by allele-specific PCR were identified in the index case and the mother. (D) The junction of the breakpoint in the allele with the intragenic deletion was confirmed by Sanger sequencing of the PCR product. Coverage and reads were drawn by the graphical user interface of Sequence Miner 5.21.1 (WuXi NextCODE).

has a heterozygous 6-kb deletion in *DOK7* encompassing exons 1 and 2.

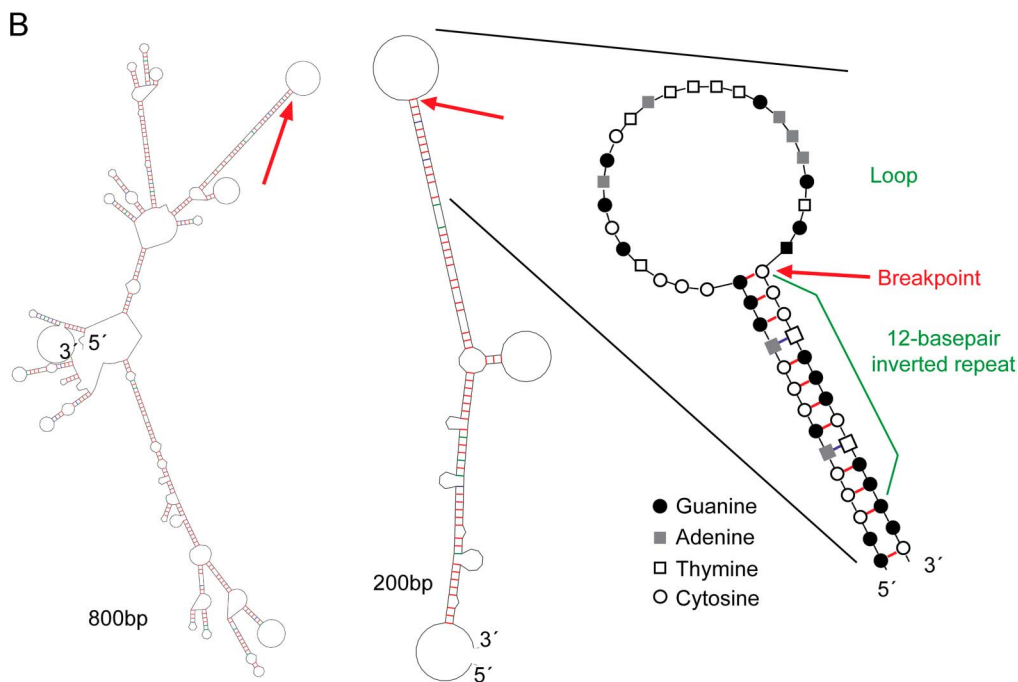
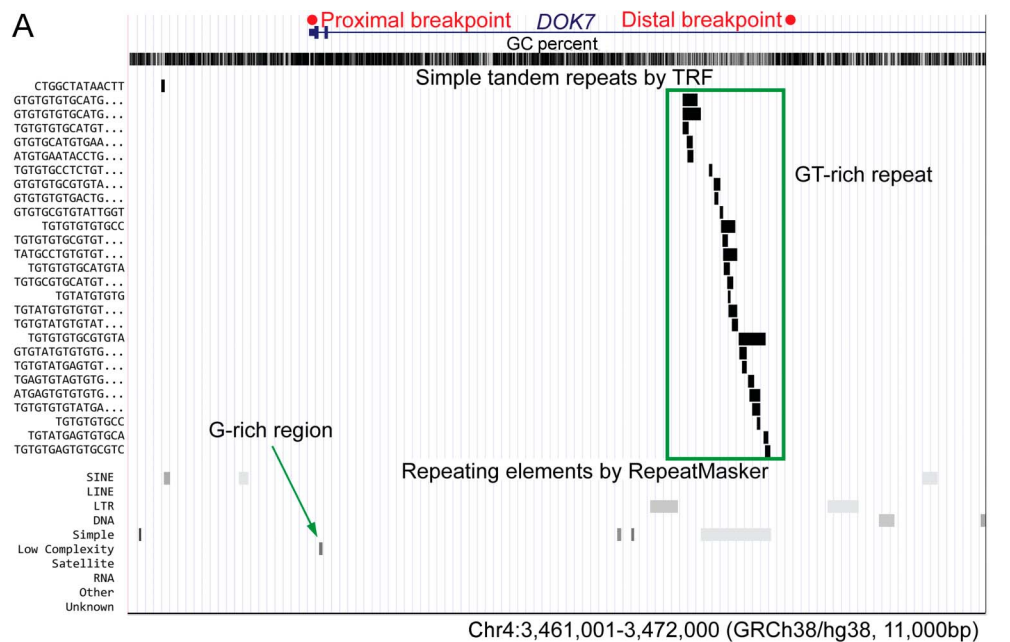
Identification and analysis of the intragenic *DOK7* deletion. We performed PCR using a pair of primers

designed around 250 bp away from the presumed breakpoints of the deletion, between the 5' untranslated region and intron 2. The expected product of 488 bp was amplified in the DNA samples of the patient, but not in control DNA

(figure 1C). The junction of the 2 breakpoints was identified by Sanger sequencing of the PCR product (figure 1D). The exact size of the deletion is 6,261 bp. The deletion was also detected by PCR

in the mother, who did not carry the c.1124_1127dup mutation. We therefore concluded that the CMS in the patient is caused by the compound heterozygous mutations in *DOK7*.

Figure 2 Analysis of the breakpoints of the intragenic 6-kb deletion



(A) University of California Santa Cruz genome browser (genome.ucsc.edu/) view of the deleted region showing the Simple Tandem Repeats track (based on Tandem Repeats Finder, TRF²⁸) and the Repeating Elements track (based on RepeatMasker¹⁹). GT-rich repeat regions (green box) are seen around the distal breakpoint, and a G-rich region (green arrow) is located near the proximal breakpoint. (B) The secondary DNA structure with the lowest delta G value was predicted by the mfold tool (unafold.rna.albany.edu/?q=mfold) for the 800 and 200 bp regions around the proximal breakpoint. An enlarged view of the breakpoint area highlighting the complementary nucleotides is also shown. The proximal breakpoint (indicated by the red arrows) is at the boundary of a loop and a 12-bp inverted repeat that may cause stalling of DNA replication. It is possible that deletion/duplication can occur if stalled replication resumes using an alternate location on the same chromosome. Red/blue/green bars represent hydrogen bonds between G-C/T-A/G-T.

The 2 breakpoints of the deletion have a C-triplet homology region, and the deleted region contains a G-rich region and GT-rich repeat region (figure 2A). In silico secondary structure analysis using the prediction program mfold¹² showed that the proximal breakpoint is at the boundary of a loop and a 12-bp inverted repeat (figure 2B). This may cause stalling of DNA replication and subsequently result in chromosomal structural changes including deletions, if replication resumes using an alternate chromosomal location.

Screening of the intragenic deletion in a CMS cohort. To identify carriers of single heterozygous mutations in *DOK7* (i.e., without a second rare variant within coding regions and exon-intron boundaries), we interrogated our database of clinically diagnosed CMS cases referred to us in the years 1996–2015. The total number of patients with CMS was 577, of which 7 genetically unsolved cases had single frameshift mutations in *DOK7* (c.1124_1127dup in 6 cases and c.1378dup in 1 case). These samples were amplified using the deletion-specific pair of primers used to detect the 6-kb deletion of the index family. All 7 samples were negative using this PCR method. This does not exclude that they carry CNVs in *DOK7* different from the one described in this study.

DISCUSSION We identified an intragenic *DOK7* deletion in a patient with clinically diagnosed CMS. Patients lacking a second heteroallelic mutation in *DOK7* were reported in a previous study.² Moreover, multiexon genomic deletions of *RAPSN*¹³ and *COLQ*¹⁴ have also been identified as causative of CMS. It is therefore conceivable that CNVs in *DOK7* may explain a proportion of cases assessed as negative or inconclusive by conventional sequencing analysis.

Our study shows the advantage of WGS analysis and detailed interrogation for detecting CNVs, using coverage and visual analysis of split reads. Traditionally, multiplex ligation-dependent probe amplification (MLPA) is considered the method of choice to detect previously described CNVs, where kits are available commercially. To identify new CNVs, however, specific MLPA primers for each gene need to be designed, rendering it expensive and time consuming for testing a genetically heterogeneous syndrome such as CMS. Array comparative genomic hybridization (aCGH) is also a valuable method for CNVs analysis; nevertheless, deletions/duplications are not detectable by aCGH if they are shorter than the spacing of the hybridization probes. In addition, neither MLPA nor aCGH can detect single nucleotide variants. Despite WES being widely used for clinical sequencing, the library preparation step results in uneven coverage, which makes the estimation

of CNVs by read depth less reliable. This can be overcome by the homogenous coverage of WGS, allowing both the detection of single nucleotide as well as CNV.

WGS analysis is still more expensive than WES and Sanger sequencing. In addition, computational tools need further improvement in sensitivity and specificity to detect CNVs exhaustively.¹⁵ Taken together, we believe that WGS is advantageous and will become the method of choice for genetic diagnosis in rare, heterogeneous conditions such as CMS. We suggest that previously unsolved cases or the carriers of a single mutation in a causal gene are especially suitable cases of CMS for WGS analysis. The 6-kb deletion was not identified in other cases tested by PCR, although it is inherited from the mother, suggesting this is likely a private mutation. However, it is possible that other CNVs in *DOK7* underlie in CMS cases.

We also determined the breakpoints of the 6-kb deletion, and analysis of the sequence and secondary structure suggested that long inverted repeats might cause the development of the deletion due to a stall of replication, and microhomology might have played a role in the repair process.¹⁶ Further documentation of breakpoints and sequences would help understand the mechanism for the development of CNVs.

Obtaining genetic diagnosis of CMS is very important because the therapy varies depending on the affected gene. Poor response to AChE inhibitors is often observed in patients affected by limb-girdle CMS due to *DOK7* mutations. Salbutamol therapy has now been started for the patient described in this study, which has been reported of good response in *DOK7*-CMS.¹⁷

AUTHOR CONTRIBUTIONS

Yoshiteru Azuma: drafting the manuscript, acquisition of data, and analysis and interpretation. Ana Töpf: analysis and interpretation and critical revision of the manuscript. Teresinha Evangelista and Paulo José Lorenzoni: acquisition of data. Andreas Roos: analysis and interpretation and study supervision. Pedro Viana: acquisition of data. Hidehito Inagaki and Hiroki Kurahashi: analysis and interpretation. Hanns Lochmüller: study concept and design and study supervision.

STUDY FUNDING

Study funded by European Commission's Seventh Framework Programme (FP7/2007-2013) under grant agreement no. 2012-305121 (NEUROMICS). Hanns Lochmüller—funding from the Medical Research Council as part of the MRC Centre for Neuromuscular Diseases (reference G1002274, grant ID 98482) and by the European Union Seventh Framework Programme (FP7/2007-2013) under grant agreement no. 305444 (RD-Connect).

DISCLOSURE

Yoshiteru Azuma, Ana Töpf, and Teresinha Evangelista report no disclosures. Paulo José Lorenzoni has received research support from CNPq (Brazil). Andreas Roos, Pedro Viana, Hidehito Inagaki, and Hiroki Kurahashi report no disclosures. Hanns Lochmüller has served on the scientific advisory boards of German Duchenne parents project, IRDiRC Interdisciplinary Scientific Committee, German Muscular Dystrophy

Network, Myotubular Trust Patient Registry, Action Duchenne Patient Registry, German Patient Registries on DMD, and SMA; has received travel funding/speaker honoraria from PTC Therapeutics Inc. and Ultragenyx Pharmaceuticals Inc.; serves on the editorial boards of the *Journal of Neuromuscular Diseases* and the *Journal of Neurology*; has been a consultant for Roche Pharmaceuticals, ASD Therapeutics Partners LLC, IOS Press, Alexion Pharmaceuticals Inc., Ultragenyx Pharmaceutical Inc., and Fondazione Cariplo (funding from each paid to Newcastle University); and has received research support from Marigold Foundation Ltd., Ultragenyx Pharmaceutical Inc., PTC Therapeutics Inc., Eli Lilly and Co., Action Benni & Co., GSK (GlaxoSmithKline), Trophos SA, European Commission (RD-Connect), European Commission (OPTIMISTIC), European Commission (NeurOmics), Medical Research Council (MRC), National Institute for Health Research (NIHR), Action Duchenne, Association Francaise Contre les Myopathies, British Heart Foundation, Muscular Dystrophy UK, National Cancer Institute, Spinal Muscular Atrophy Support UK, Wellcome Trust, Jennifer Trust, and Duchenne Parent Project. Go to Neurology.org/ng for full disclosure forms.

Received January 19, 2017. Accepted in final form March 14, 2017.

REFERENCES

- Engel AG, Shen XM, Selcen D, Sine SM. Congenital myasthenic syndromes: pathogenesis, diagnosis, and treatment. *Lancet Neurol* 2015;14:420–434.
- Beeson D, Higuchi O, Palace J, et al. Dok-7 mutations underlie a neuromuscular junction synaptopathy. *Science* 2006;313:1975–1978.
- Das AS, Agamanolis DP, Cohen BH. Use of next-generation sequencing as a diagnostic tool for congenital myasthenic syndrome. *Pediatr Neurol* 2014;51:717–720.
- Garg N, Yiannikas C, Hardy TA, et al. Late presentations of congenital myasthenic syndromes: how many do we miss? *Muscle Nerve* 2016;54:721–727.
- Bauche S, O'Regan S, Azuma Y, et al. Impaired presynaptic high-affinity choline transporter causes a congenital myasthenic syndrome with episodic apnea. *Am J Hum Genet* 2016;99:753–761.
- O'Connor E, Topf A, Muller JS, et al. Identification of mutations in the MYO9A gene in patients with congenital myasthenic syndrome. *Brain* 2016;139:2143–2153.
- Lelieveld SH, Spielmann M, Mundlos S, Veltman JA, Gilissen C. Comparison of exome and genome sequencing technologies for the complete capture of protein-coding regions. *Hum Mutat* 2015;36:815–822.
- Li H, Durbin R. Fast and accurate long-read alignment with Burrows-Wheeler transform. *Bioinformatics* 2010;26:589–595.
- Picard. Available at: broadinstitute.github.io/picard/. Accessed March 23, 2017.
- McKenna A, Hanna M, Banks E, et al. The Genome Analysis Toolkit: a MapReduce framework for analyzing next-generation DNA sequencing data. *Genome Res* 2010;20:1297–1303.
- Auton A, Brooks LD, Durbin RM, et al. A global reference for human genetic variation. *Nature* 2015;526:68–74.
- Zuker M. Mfold web server for nucleic acid folding and hybridization prediction. *Nucleic Acids Res* 2003;31:3406–3415.
- Gaudon K, Penisson-Besnier I, Chabrol B, et al. Multiexon deletions account for 15% of congenital myasthenic syndromes with RAPSN mutations after negative DNA sequencing. *J Med Genet* 2010;47:795–796.
- Wang W, Wu Y, Wang C, Jiao J, Klein CJ. Copy number analysis reveals a novel multiexon deletion of the *COLQ* gene in congenital myasthenia. *Neurol Genet* 2016;2:e117. doi: 10.1212/NXG.0000000000000117.
- Pirooznia M, Goes FS, Zandi PP. Whole-genome CNV analysis: advances in computational approaches. *Front Genet* 2015;6:138.
- Hastings PJ, Ira G, Lupski JR. A microhomology-mediated break-induced replication model for the origin of human copy number variation. *PLoS Genet* 2009;5:e1000327.
- Lorenzoni PJ, Scola RH, Kay CS, et al. Salbutamol therapy in congenital myasthenic syndrome due to DOK7 mutation. *J Neurol Sci* 2013;331:155–157.
- Benson G. Tandem repeats finder: a program to analyze DNA sequences. *Nucleic Acids Res* 1999;27:573–580.
- Smit A, Hubley R, Green P. RepeatMasker Open-3.0. 1996–2010. Available at: repeatmasker.org. Accessed March 23, 2017.